Large-scale coherence in assemblies of self-propelled bioparticles: from shaken rods to swimming bacteria

Igor Aronson

Materials Science

Argonne National Laboratory

Andrey Sokolov, *IIT & ANL*
Ray Goldstein, *U Arizona/Cambridge*
John Kessler, *U Arizona*
Lev Tsimring, *UCSD*
Dmitry Volfson, *UCSD*

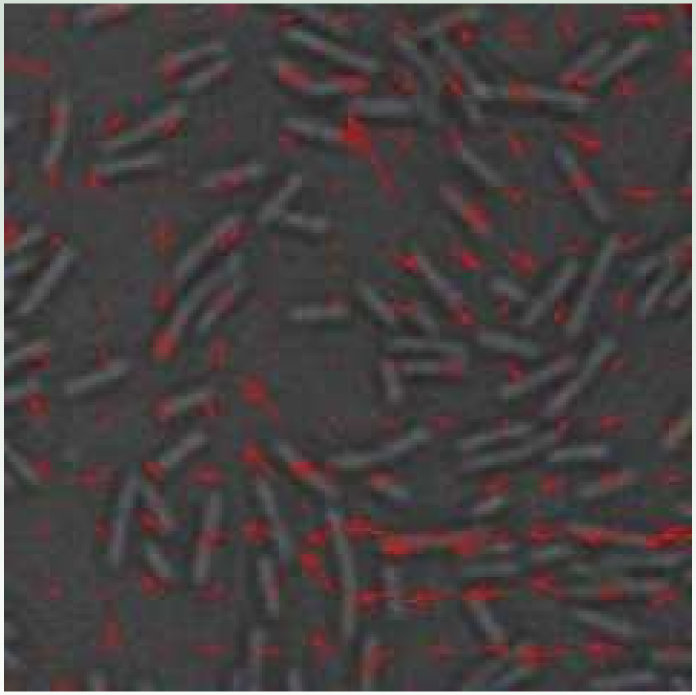

Supported by US Department of Energy

Outline

- Experiments on bacteria (polar particles)
- Theoretical concepts (inelastic polar rods)
- Swirling of “apolar particels”
- Polarization of “active nematic” and swirling instability

Long-Range Order in System of Self-Propelled Particles

Gregoire & Chate, PRL 2004
Helbing, Farkas, Vicsek, Nature (2000)
Ramaswami et al

- Particles move with constant speed
- Align directions with neighbors
- Competition between alignment and noise
- Complex emergent behavior originates from simple rules
- Anomalous fluctuations, phase transitions
- Birds flocks, fish schools, elephant/moutons herds, nano-robots swarms
- Very stimulating but totally uncontrolled experiments

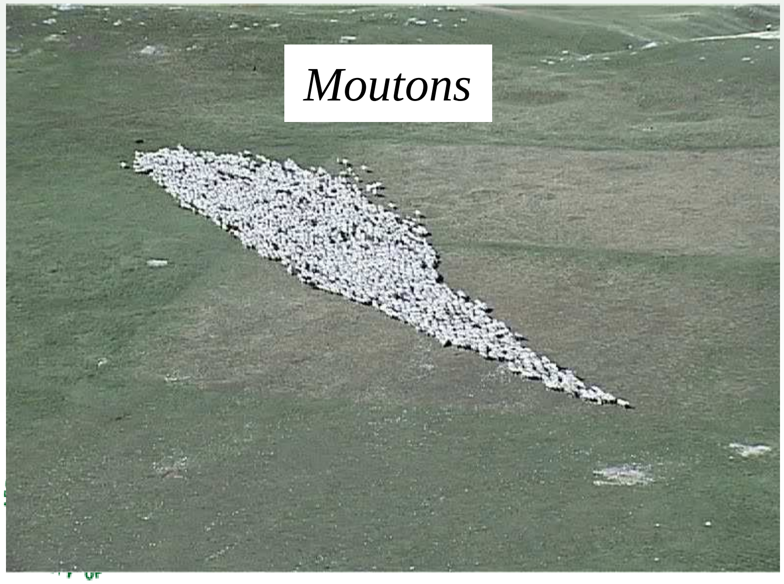

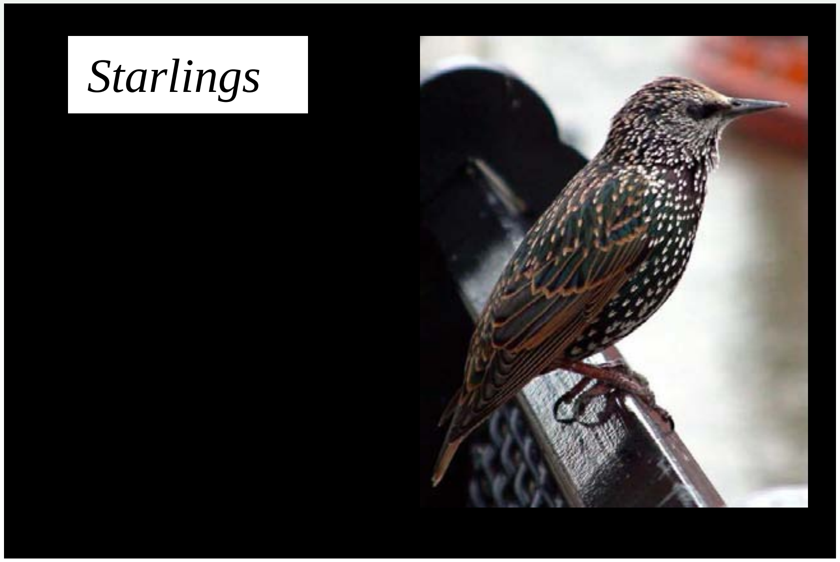

Self-organized emergent behavior

Cytoskeleton (Microtubules, motors)
Nedelec et al

Shaken rice at Argonne

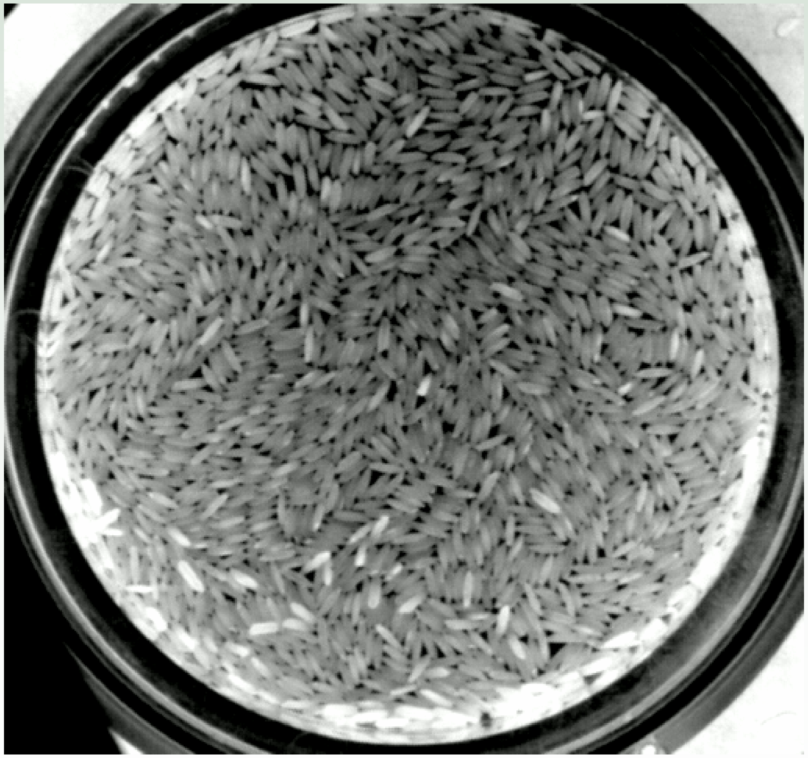

Self-Propelled BioParticles

- swimming bacteria *Bacillus Subtilis*
- length 5 μm, speed 20 μm/sec
- collective flows up to 100 μm/sec

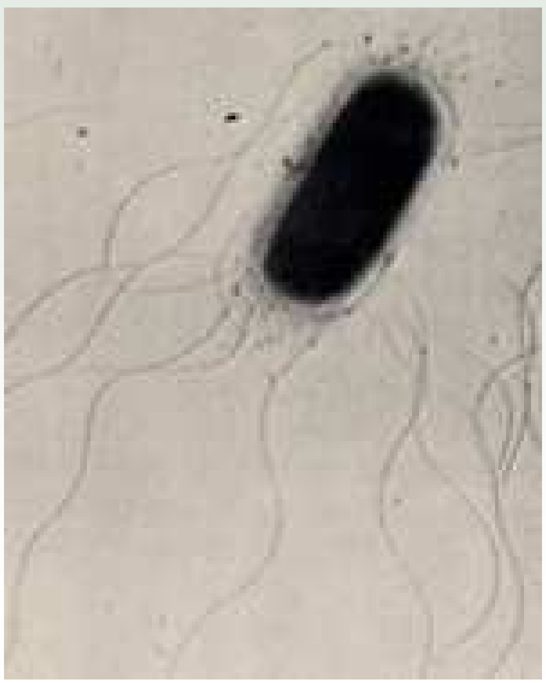

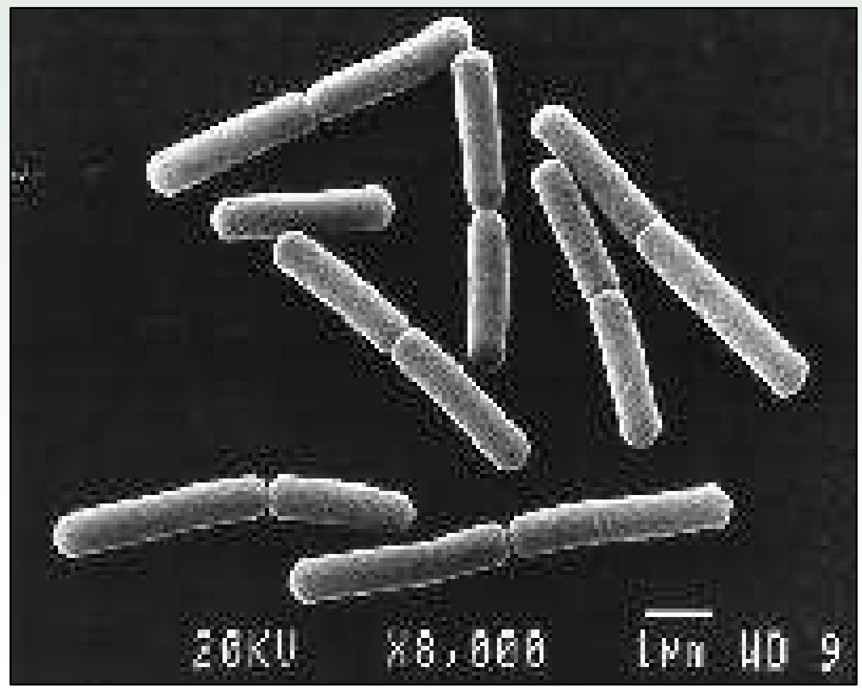

Complicated Machines

Bacterial Structures

- Flagella
- Pili
- Capsule
- Plasma Membrane
- Cytoplasm
- Cell Wall
- Lipopolysaccharides
- Teichoic Acids
- Inclusions
- Spores

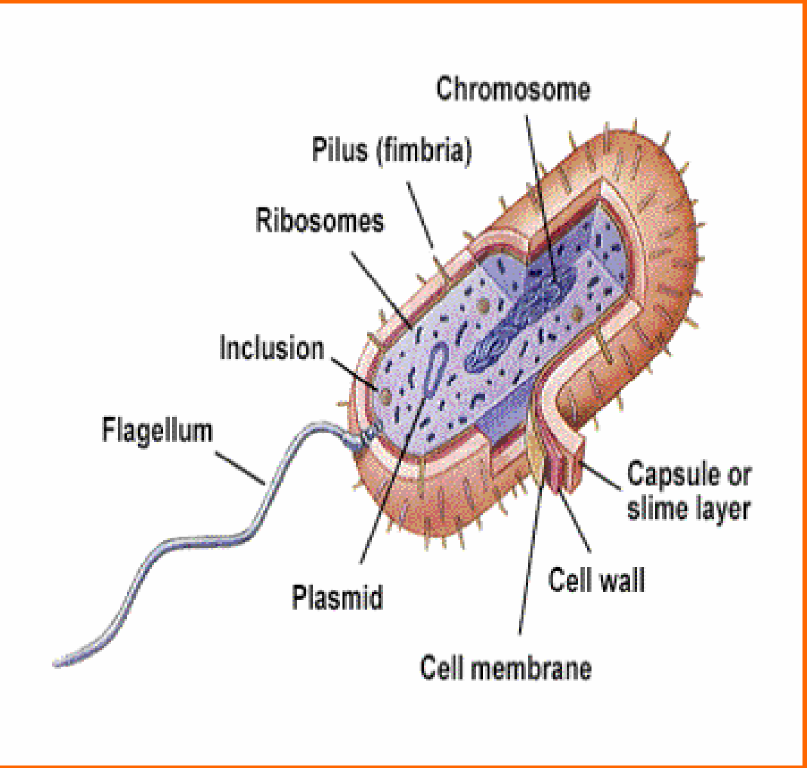

Chapter 4

Bio-Convection and Large-Scale Coherence in “Flat” Sessile Drop

Bugs concentrate at the contact line

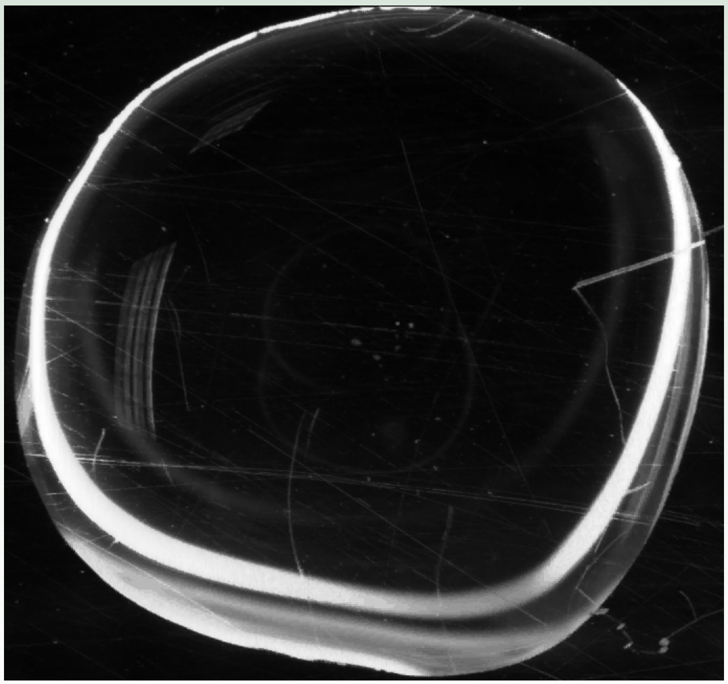

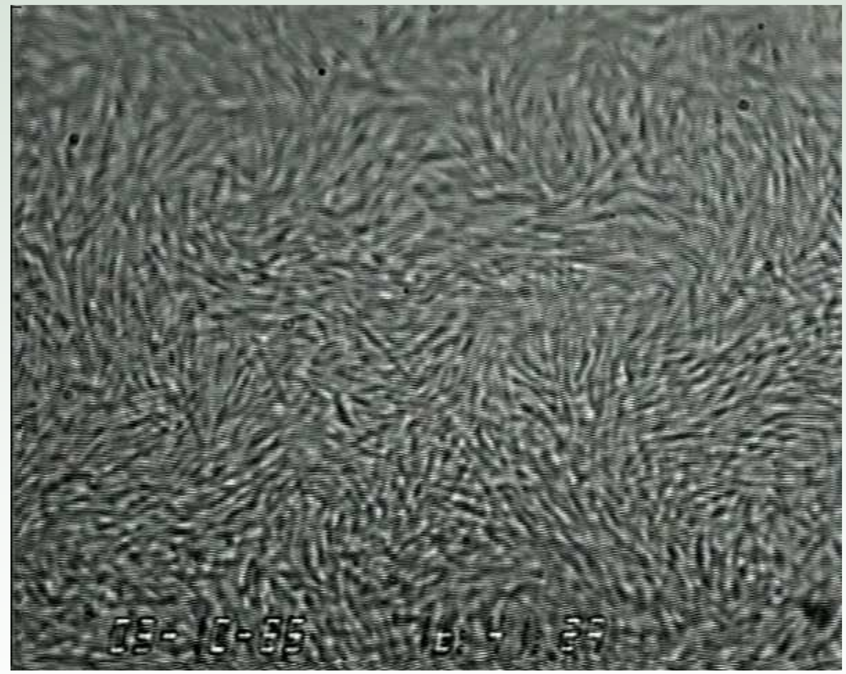

Dombrowski, Cisneros,Chatkaew, Goldstein, Kessler, PRL (2004)

Velocity Correlation Functions

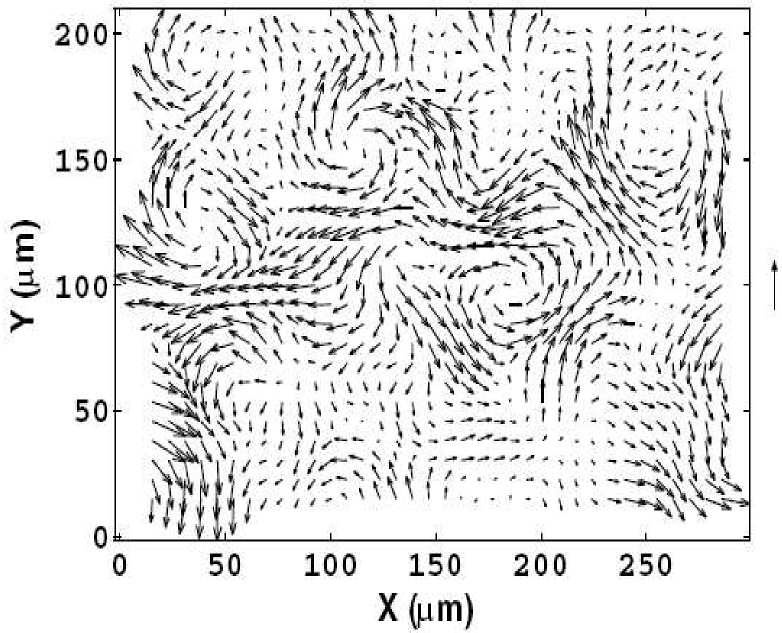

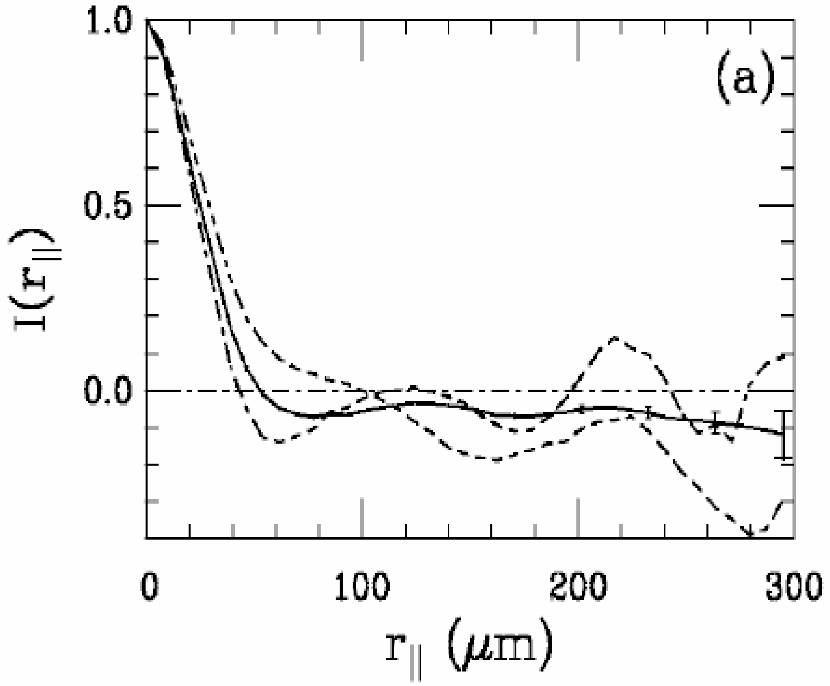

Large-Scale Coherence – pure hydrodynamic interaction

Simulations of Swimming Dimers

Michael Graham, PRL (2005)

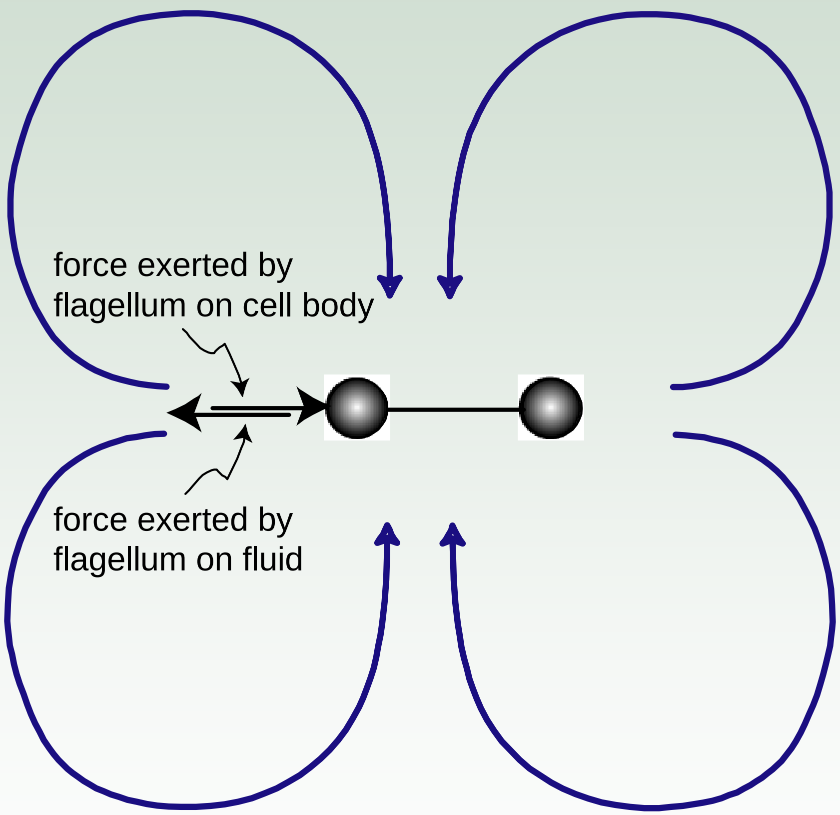

- Body: bead-rod dumbbell, length, ℓ bead friction ζ
- "Phantom" flagellum
  - exerts equal and opposite forces f on body and fluid along axis of body
- No excluded volume except at walls
- Point-force low-Re hydrodynamics
- Neutrally buoyant

$\Rightarrow$ Far field flow is a stresslet

effective volume fraction: $\phi_e = n\frac{4\pi}{3}\left(\frac{\ell}{2}\right)^3$

isolated swimmer speed: $v_{sw} = \frac{f}{2\zeta}$

Animation of Swimming Dimers

Onset of Coherence at Large Density

(from Michael Graham)

Swimmer and tracer velocities (2H = 5)

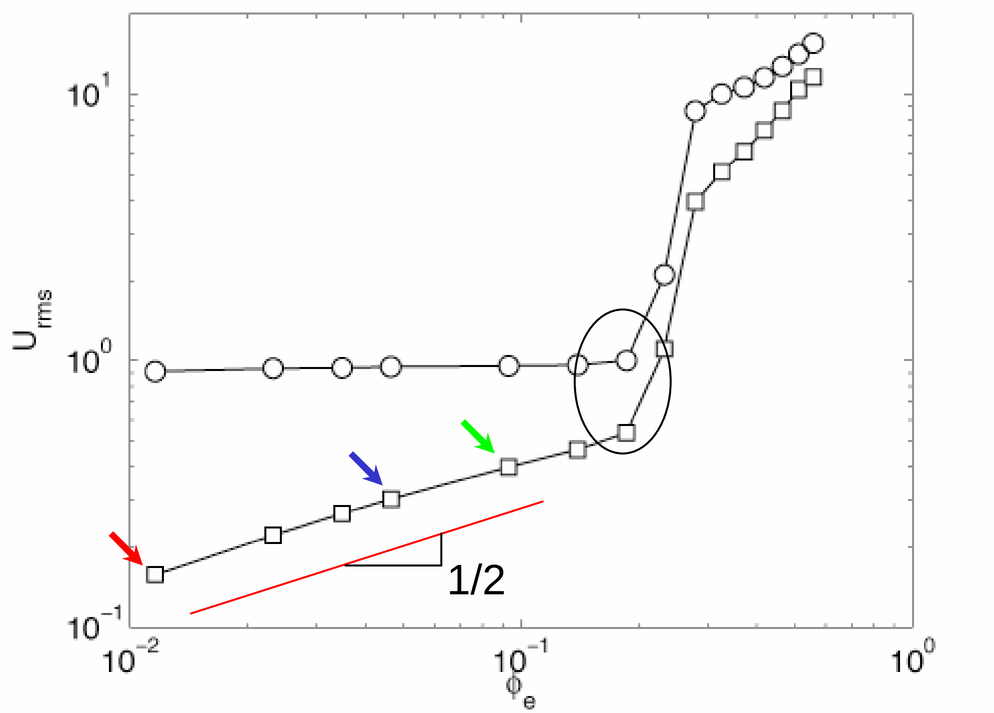

Distinct onset of large velocities:
$u_{tracer} \sim u_{swimmer}$ at transition

- Length scale increases
- At large concentration, fluctuations span the box.

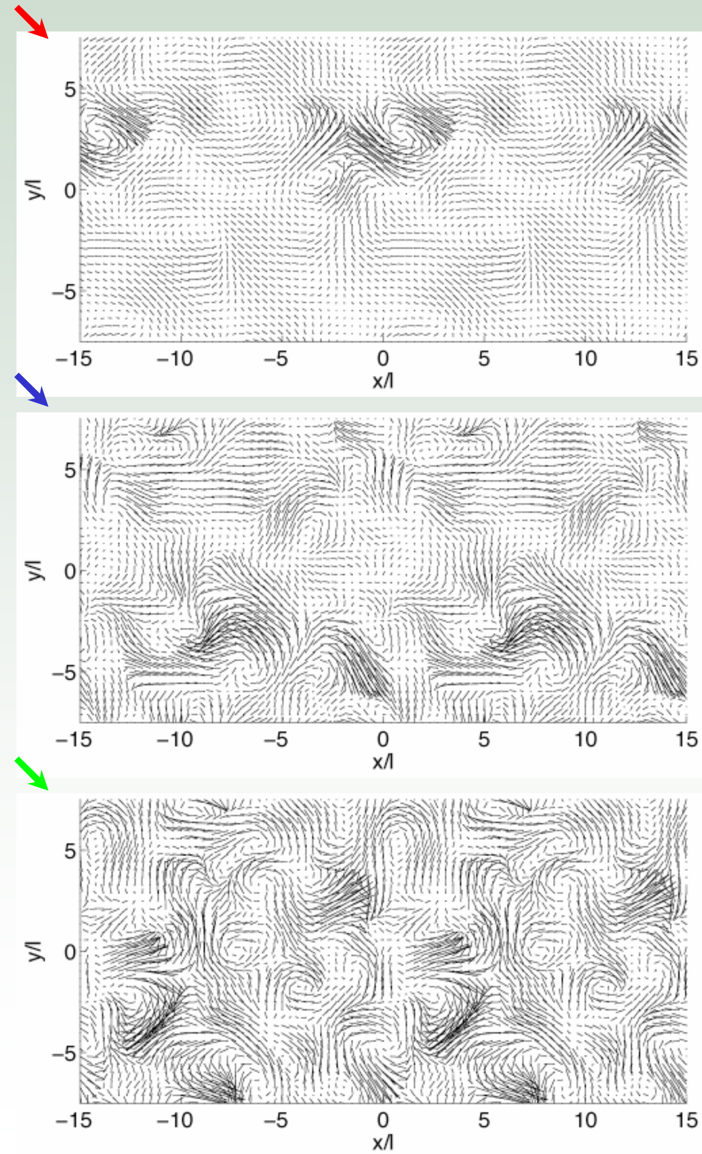

Wu & Libchaber Experiment: Film Geometry

Experimental Setup (E. coli)

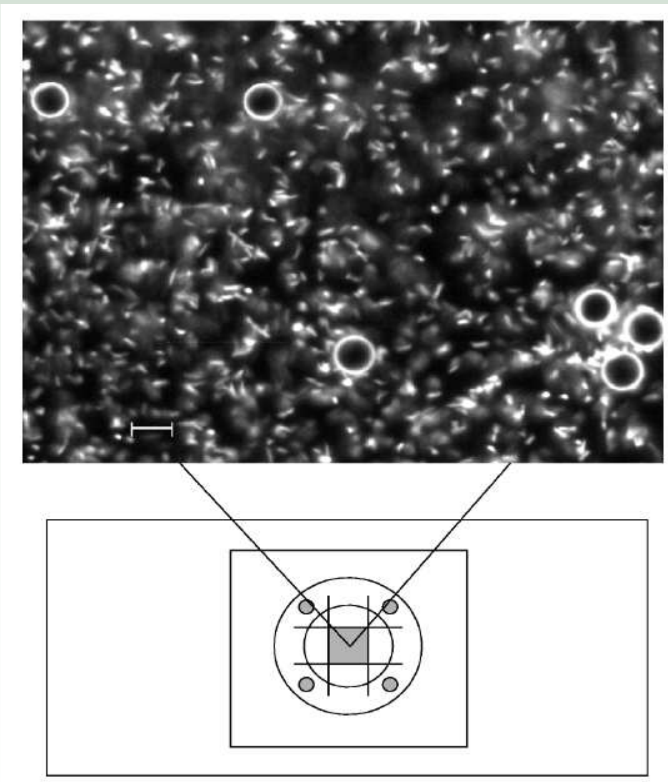

Regular diffusion – low density
Levi flights – high density

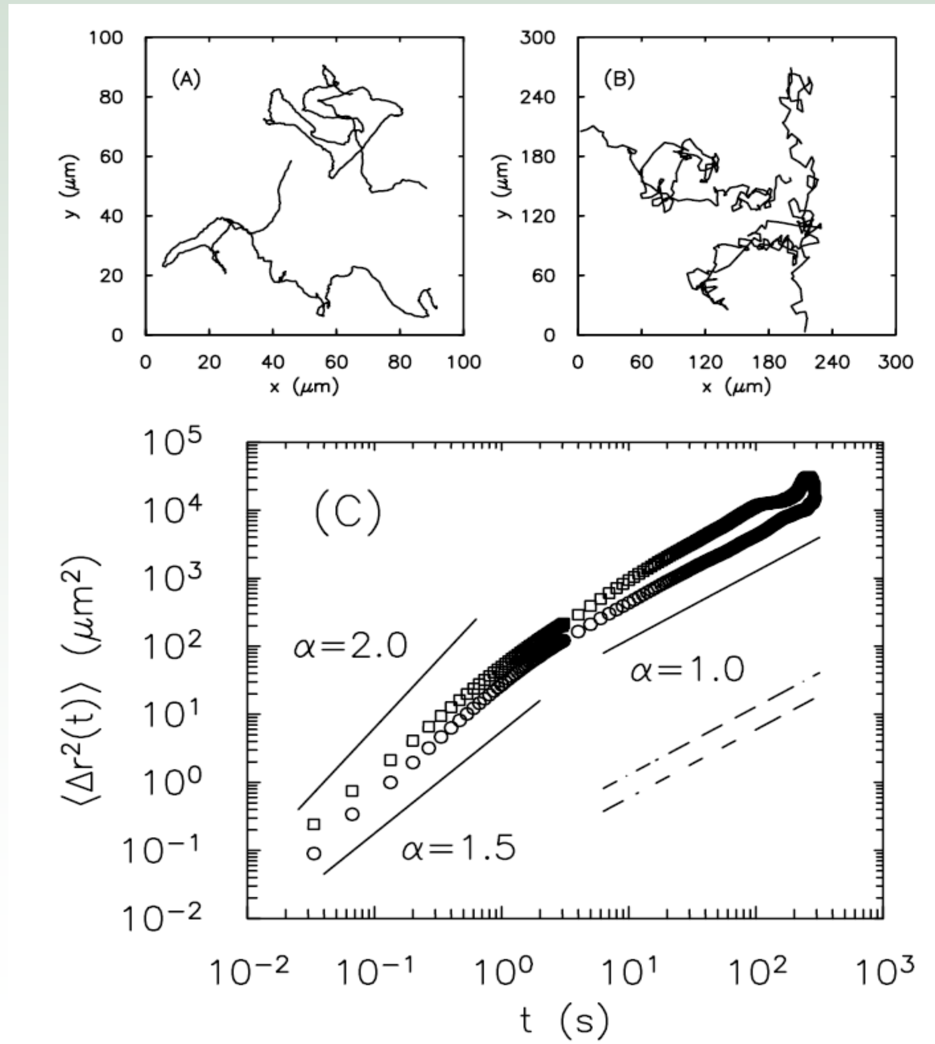

PRL (2000)

New Generation of Experiments

- Thin free-hanging film concept (Wu & Libchaber) but with important modifications
- Adjustable thickness
- Adjustable concentration of bugs

Schematics of Experimental Setup

Concept: Andrey Sokolov et al, ***ANL invention 2007***

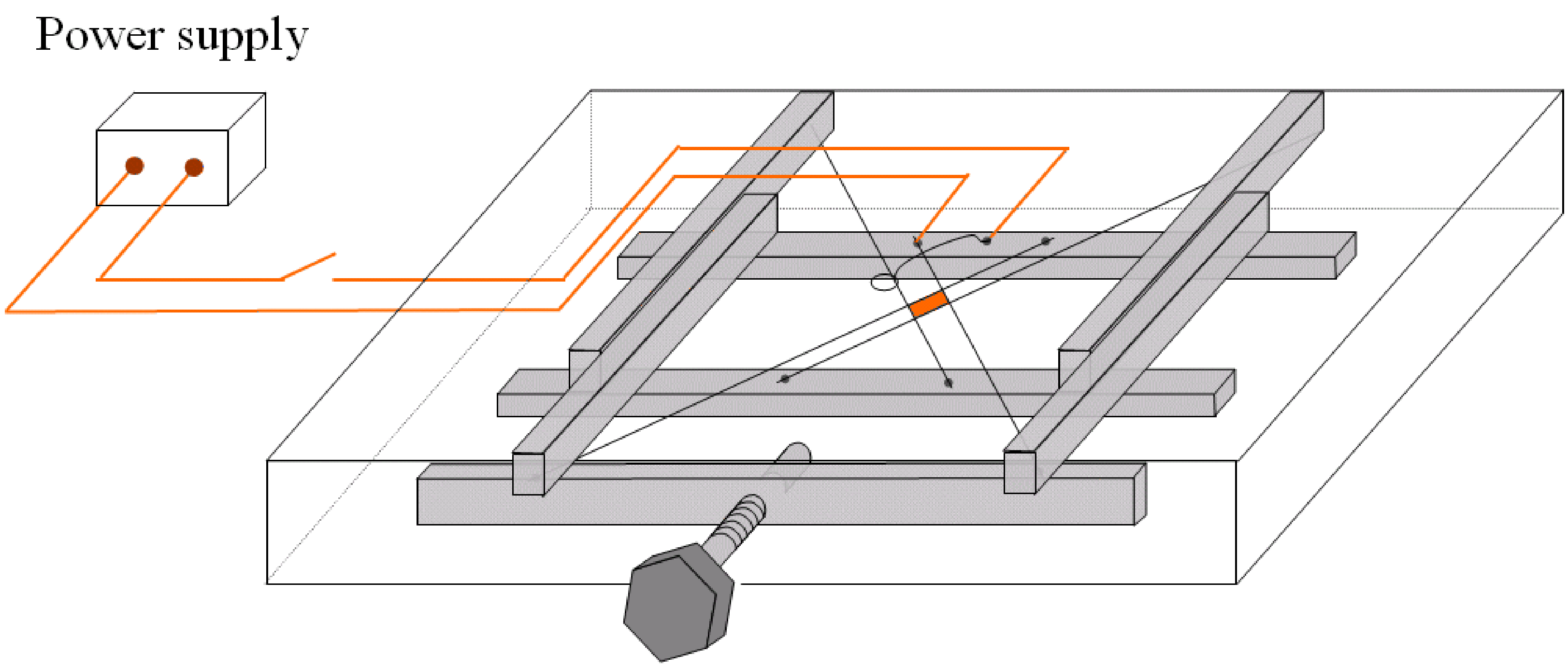

Film reduced thickness (up to 1 micron)

pH-Taxis & concentration of cells

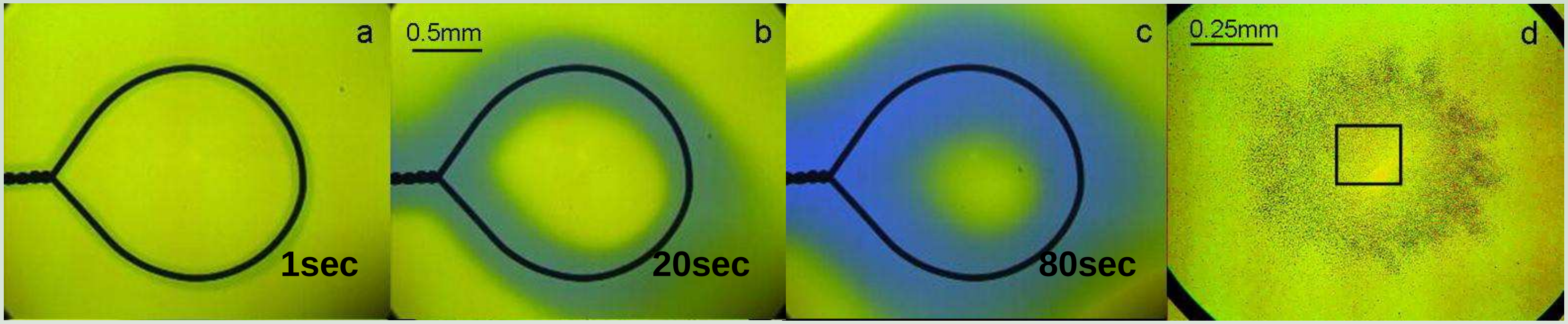

pH indicator (bromothynol blue) was added

field of view

density vs. time

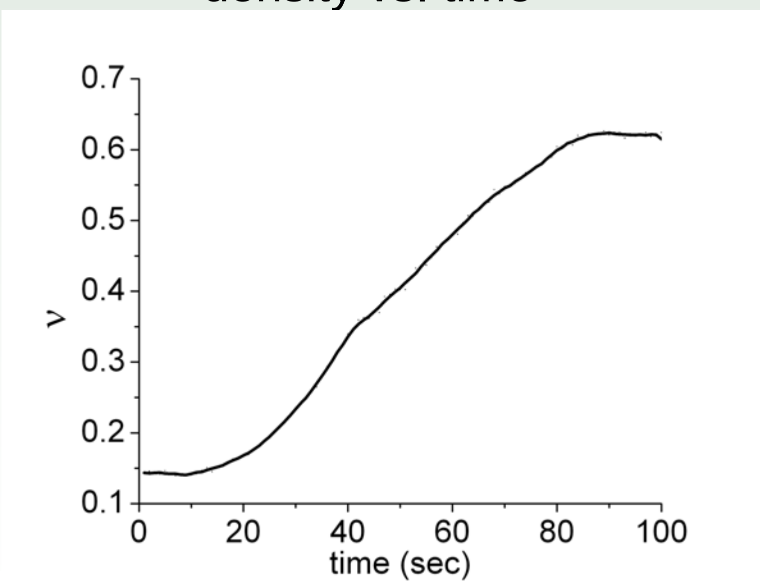

Concentrated bacteria

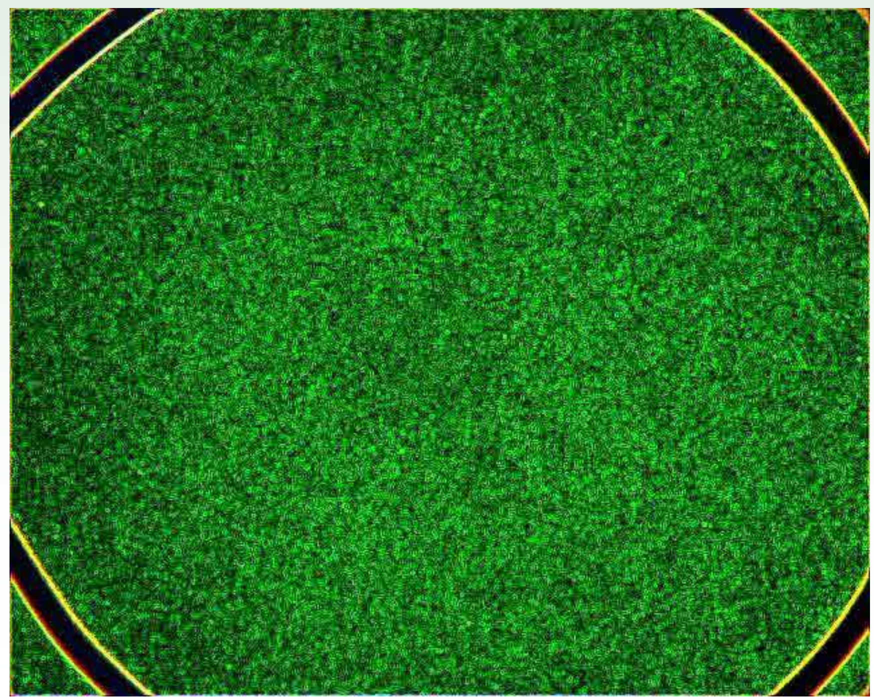

Inelastic collisions between bacteria

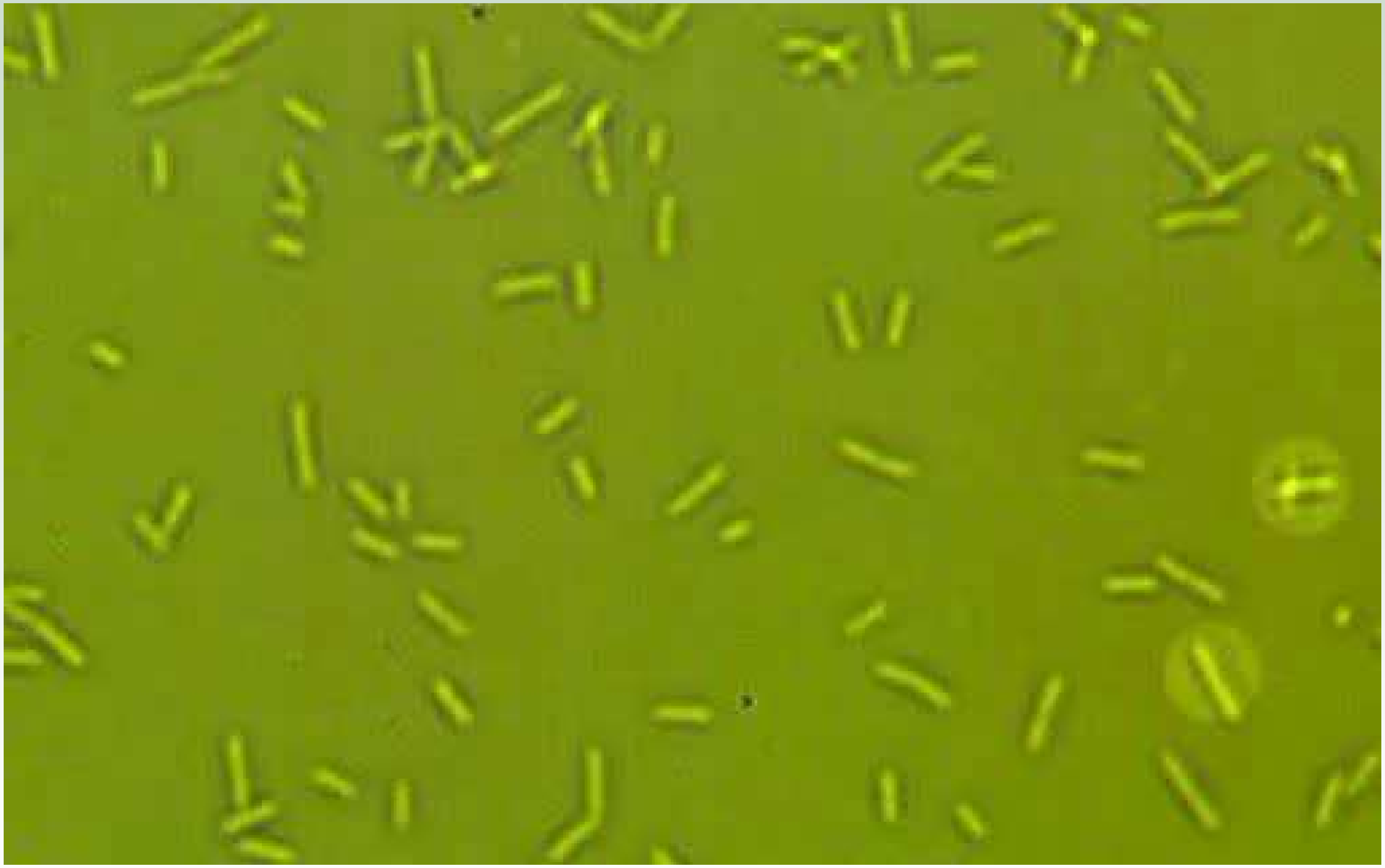

Andrey Sokolov & Igor Aranson, ANL
Ray Goldstein & John Kessler, U Arizona

Collective Swimming: High Density

BIV- BioParticles-Image Velocimetery

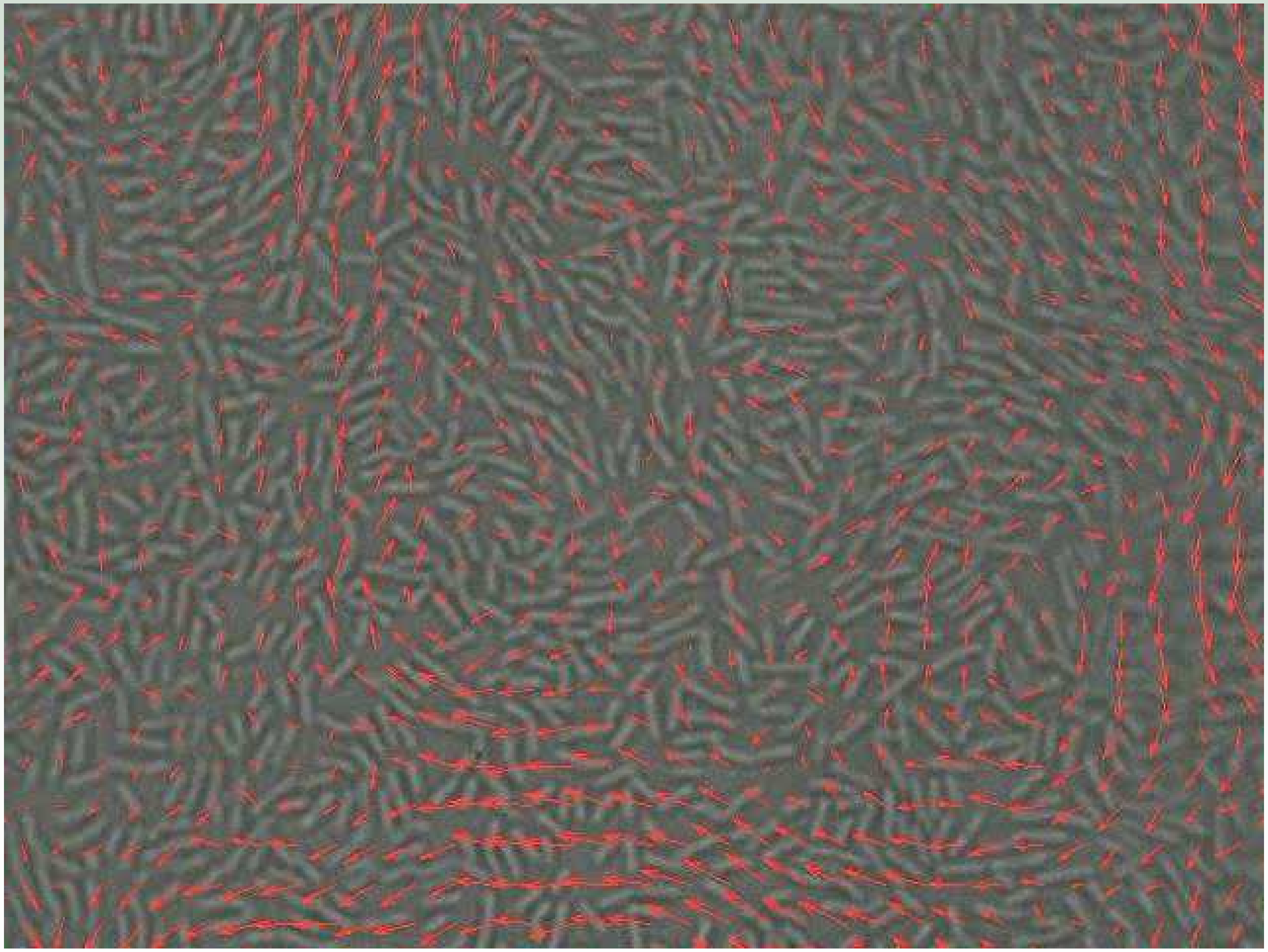

No Apparent Velocity-Orientation Correlation

Velocity Field ***V***

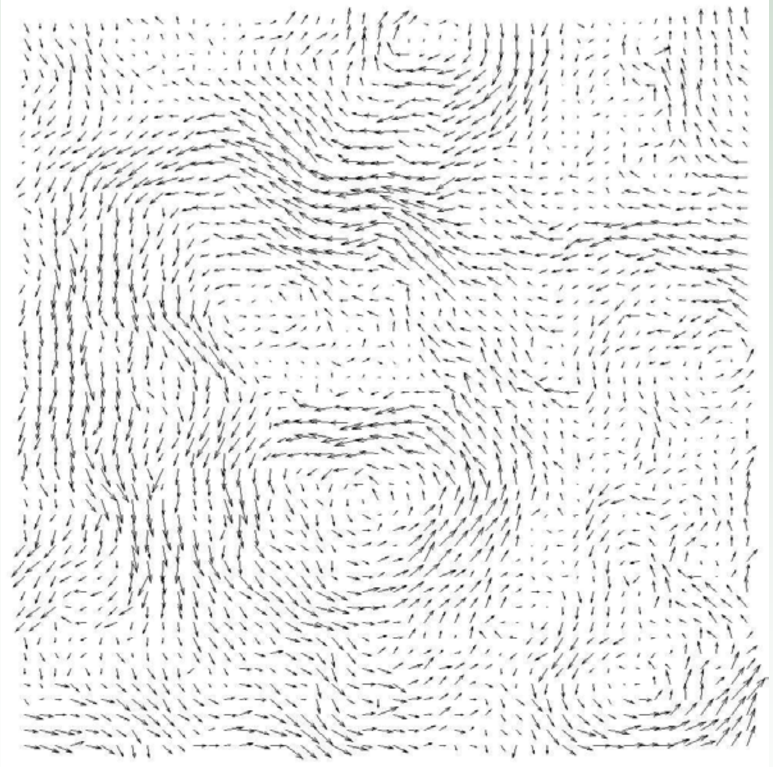

Orientation Field $\boldsymbol{\tau}$

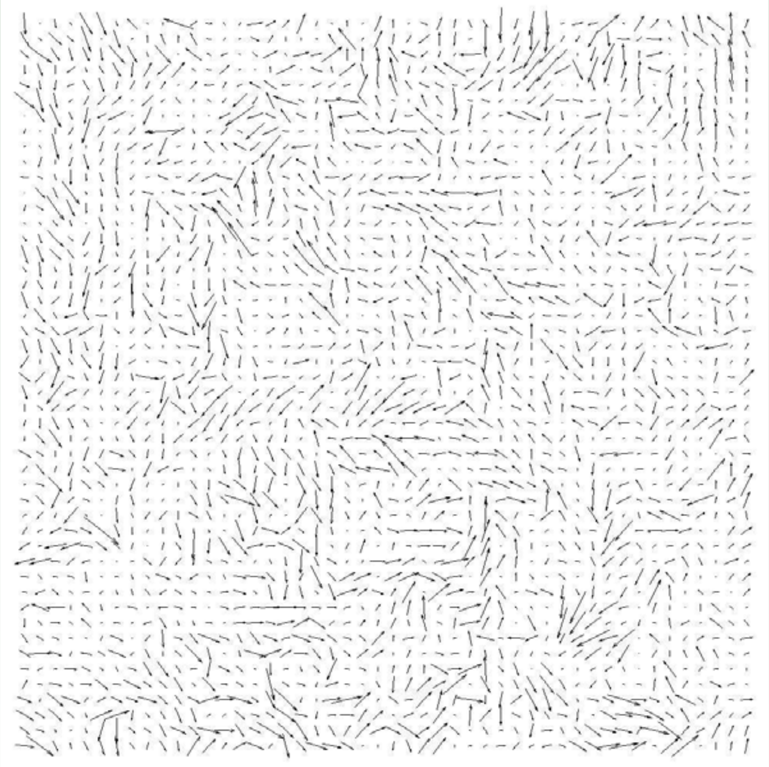

$$\frac{\langle V\tau\rangle}{\sqrt{\langle V^2\rangle\langle\tau^2\rangle}} \approx 0.03 - 0.05 \text{ - no apparent correlation}$$

Velocity-Orientation Correlation Recovered

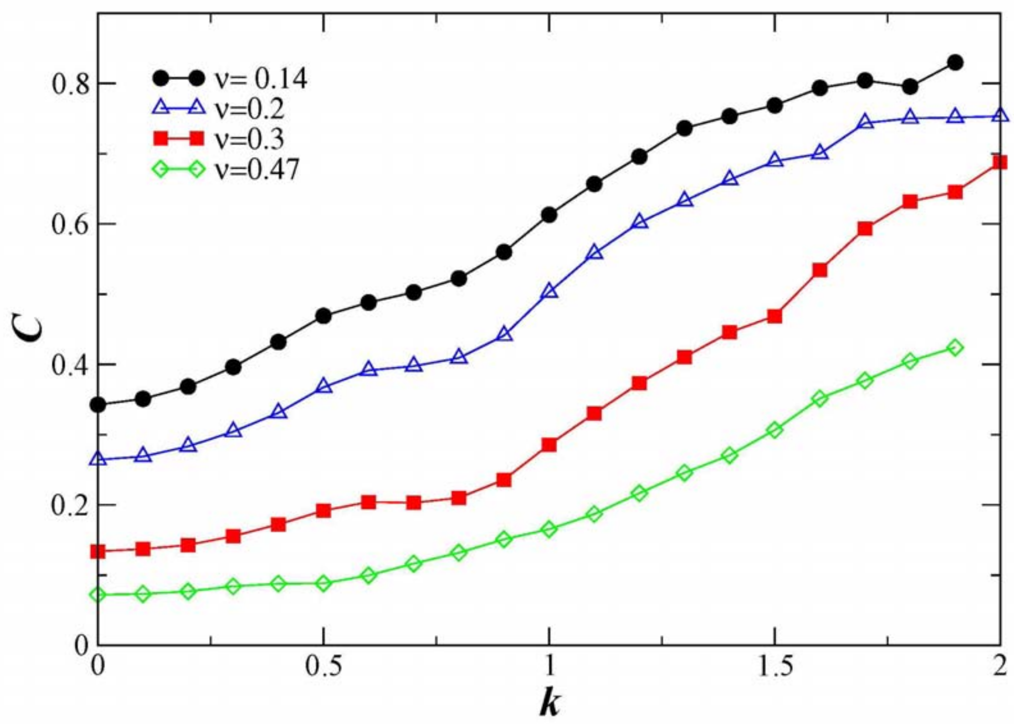

$$C(k) = \frac{\langle \cos\phi \rangle_k - 2/\pi}{1 - 2/\pi} - \text{alignmnet coefficient}$$

ϕ - angle between $\mathbf{V}$ and $\boldsymbol{\tau}$; k – threshold with respect to typical value

Transition to Collective Swimming

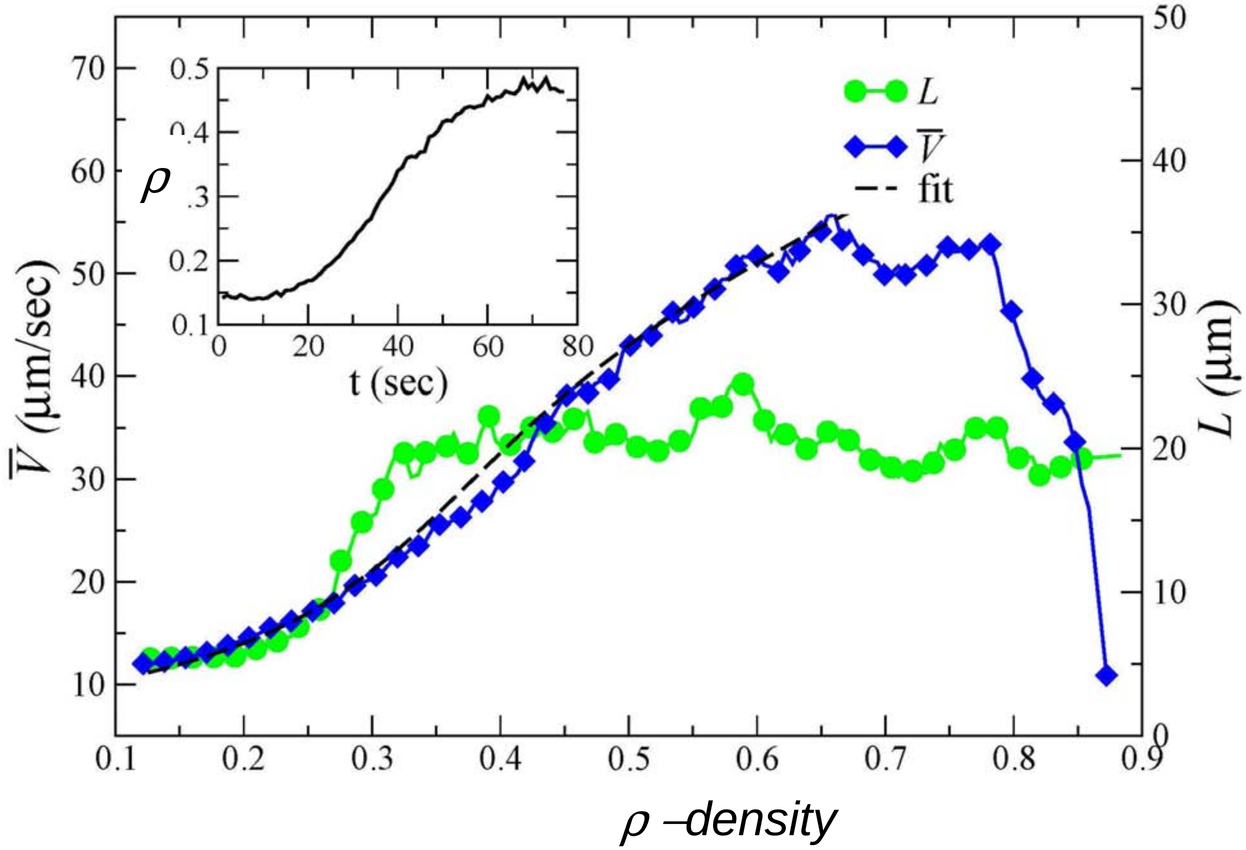

ρ-density

$\overline{\mathrm{V}}$-rms velocity

L-correlation length

$$Fit: \quad \frac{\partial V}{\partial t} = (\rho - \rho_c)V - V^3 + \eta(t)$$

Theoretical Model

- Microscopic interaction rules:

  -self-propulsion; hydrodynamically-induced inelastic collision/excluded volume

  -flow advection; direction realignment in shear flow

Inelastic collision of two bacteria

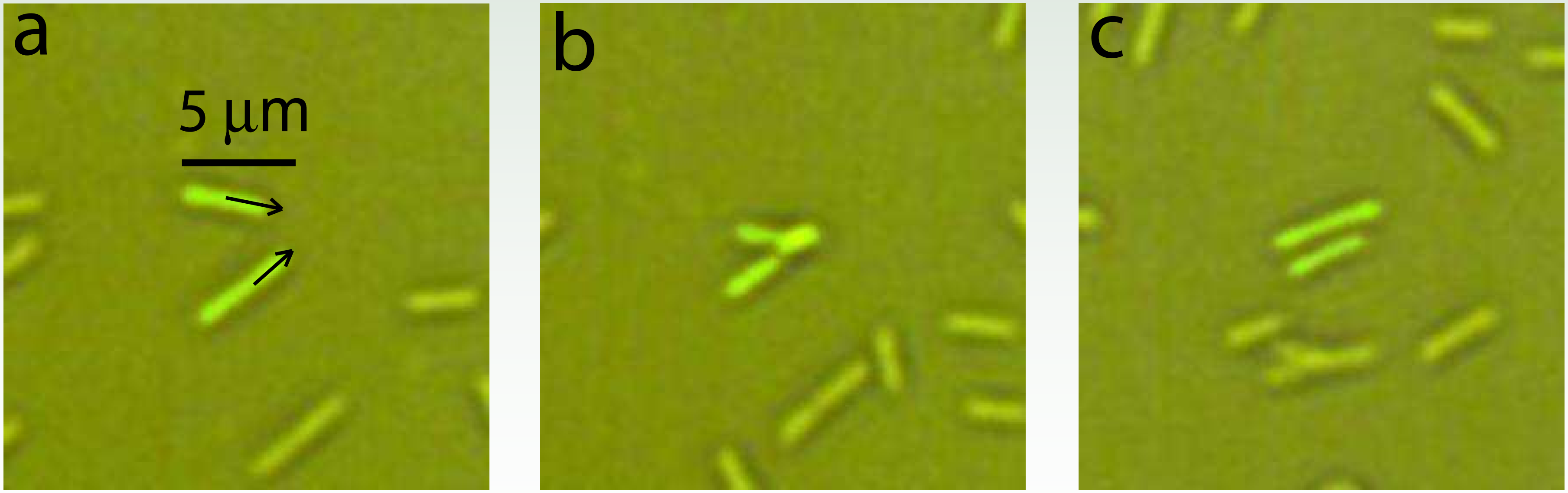

Maxwell Model for Inelastic Particles

inelastic grains

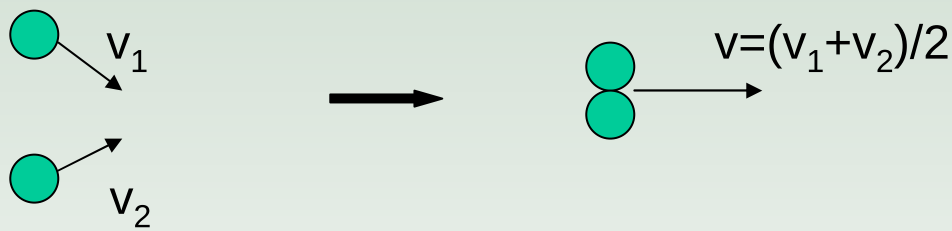

$$\begin{pmatrix} v_1^a \\ v_2^a \end{pmatrix} = \begin{pmatrix} \gamma & 1-\gamma \\ 1-\gamma & \gamma \end{pmatrix} \begin{pmatrix} v_1^b \\ v_2^b \end{pmatrix}$$

v^a & v^b velocities after/before collision

$\gamma=0$ – elastic collisions

$\gamma=1/2$ – fully inelastic collision

$\gamma=1$ – no interaction

Probability distributions *P(v)*

- Collision rate *g* does not depend on relative velocity (Maxwell molecules)
- No spatial dependence
- *D*- thermal diffusion, *D* ~*T*, *T* – temperature of heat bath
- Binary uncorrelated fully inelastic collisions

- ***Asymptotic distribution P(v) is localized but not Gaussian, the width depends on the temperature***
- ***No phase transition, the diffusion can be scaled out***

source term *sink term*

$$\frac{\partial P(v)}{\partial t} = D\frac{\partial^2 P(v)}{\partial v^2} + g\int_{-\infty}^{\infty} du_1 \int_{-\infty}^{\infty} du_2 P(u_1)P(u_2)\left[\delta(v-(u_1+u_2)/2) - \delta(v-u_2)\right]$$

heat bath

Ben-Naim & Krapivsky, PRE 2000

Results for Maxwell Model

- Nice toy model: solution can be obtained analytically by the Fourier Transform of *P(v)*
- Asymptotic distribution *P(v)* is localized but not Gaussian, the width depends on the temperature
- No phase transition, the diffusion can be scaled out

$$\text{for} \quad \gamma = \tfrac{1}{2}$$

$$\frac{\partial P(v)}{\partial t} = \frac{\partial^2 P(v)}{\partial v^2} + \int_{-\infty}^{\infty} du \left[P(v + \tfrac{1}{2}u) P(v - \tfrac{1}{2}u) - P(v) P(v - u) \right]$$

Inelastic Collision of Polar Rods

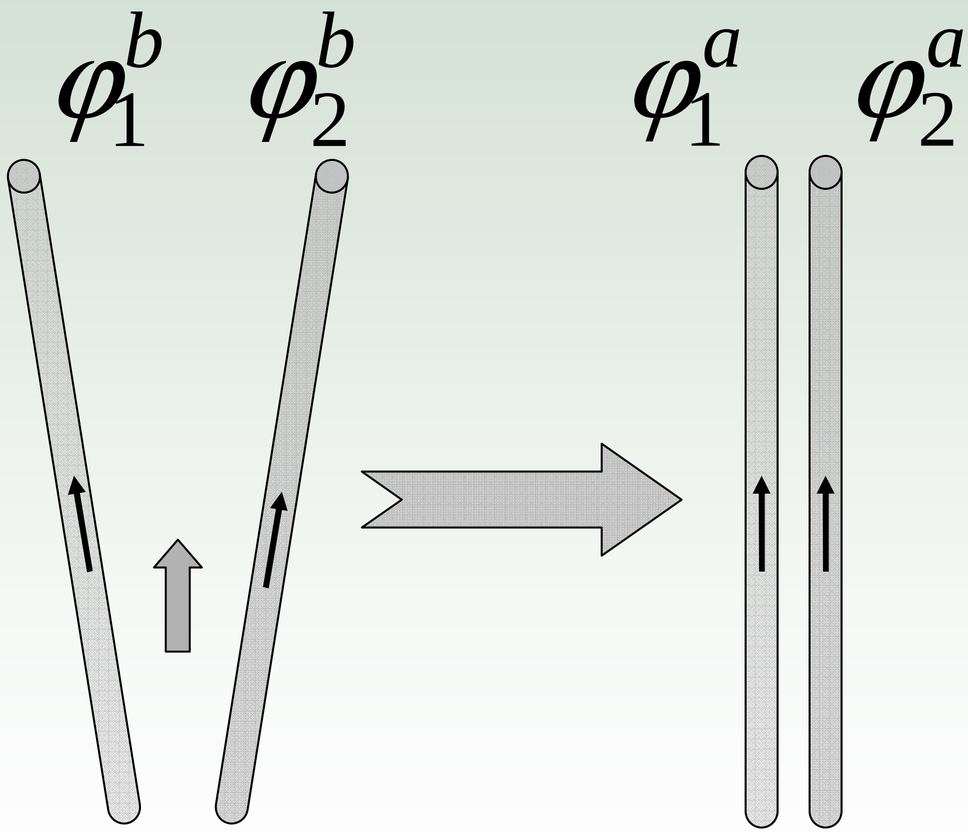

$$\varphi_1^a = \varphi_2^a = \frac{1}{2}\left(\varphi_1^b + \varphi_2^b\right)$$

$\varphi_{1,2}$ – orientation angles

Fully Inelastic Collision!!!

Probability distributions *P(φ)*

- D_r - thermal rotational diffusion
- *g=const* – collision cross-section

$$\frac{\partial P(\varphi)}{\partial t} = D_r \frac{\partial^2 P(\varphi)}{\partial \varphi^2} + g \int_{-\pi}^{\pi} du \left[P(\varphi + \tfrac{1}{2}u) P(\varphi - \tfrac{1}{2}u) - P(\varphi) P(\varphi - u) \right]$$

- Main difference – integration over finite interval due to 2π periodicity of the angle
- Orientation instability with the increase of *g*!!!

Macroscopic Variables

- Density of MT $\rho = 2\pi\left\langle P(\varphi)\right\rangle = \int_{-\pi}^{\pi} P(\varphi)d\varphi$

- Average orientation $\tau=(\tau_x,\tau_y)$

$$\tau_x = \tfrac{1}{2\pi}\int_{-\pi}^{\pi} \cos\varphi P(\varphi)d\varphi \qquad \tau_y = \tfrac{1}{2\pi}\int_{-\pi}^{\pi} \sin\varphi P(\varphi)d\varphi$$

- "Complex orientation" $\psi = \tau_x + i\tau_y = \tfrac{1}{2\pi}\int_{-\pi}^{\pi} e^{i\varphi}P(\varphi)d\varphi$

Coarse-Grained Equation

- Rigorous bifurcation analysis

$$\frac{\partial \rho}{\partial t} = 0$$

$$\frac{\partial \boldsymbol{\tau}}{\partial t} = \left((\tfrac{4}{\pi} - 1)\rho - 1 \right) \boldsymbol{\tau} - \frac{16\pi}{3(4+\rho)} |\boldsymbol{\tau}|^2 \boldsymbol{\tau}$$

- Second order phase transition

for $\rho > \rho_c = 1/0.273 \approx 3.662$

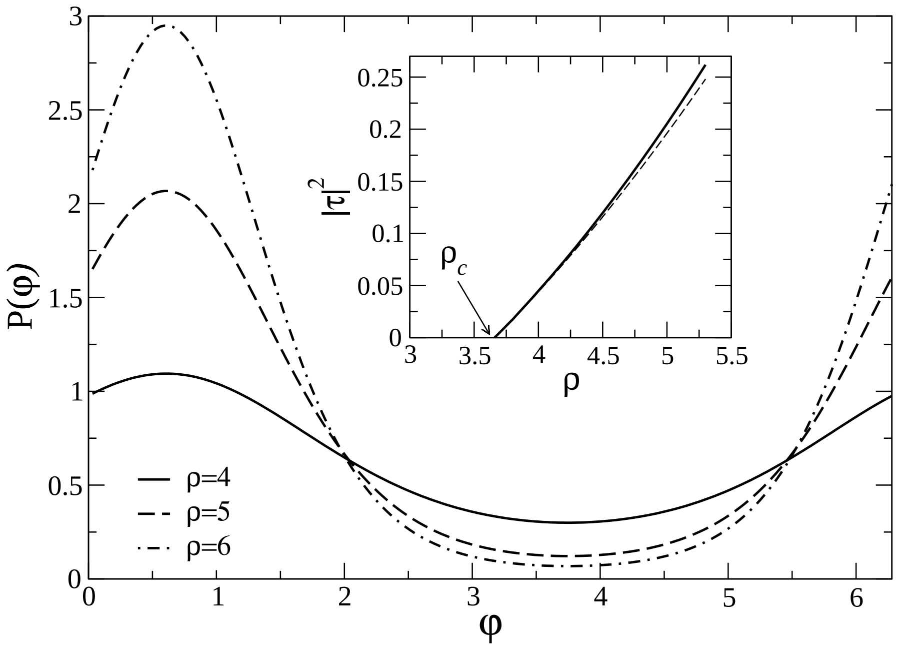

Spatial Localization of Interaction

- W- interaction kernel, interaction between rods decay with the distance
- D_{ij},D_r -translational and rotational diffusion of rods
- v_0 - propulsion velocity
- v,Ω – hydrodynamic velocity and vorticity
- E – strain rate tensor

$$\begin{aligned}\partial_t P \quad &+ \quad \nabla \cdot \left[\left(v_0 \mathbf{n} + \mathbf{v}\right) P\right] + \frac{1}{2}\Omega \partial_\phi P = D_r \partial_\phi^2 P + \partial_i D_{ij} \partial_j P + \iint d\mathbf{r_1} d\mathbf{r}_2 \int_{-\pi}^{\pi} d\phi_2 \\ &\times \quad W(\mathbf{r}_1, \mathbf{r}_2) P(\mathbf{r_1}, \phi_1) P(\mathbf{r_2}, \phi_2) \left[\delta\left(\bar{\mathbf{r}} - \mathbf{r}, \bar{\phi} - \phi\right) - \delta\left(\mathbf{r}_2 - \mathbf{r}, \phi_2 - \phi\right)\right] - \gamma \left(\mathbf{E} \cdot \mathbf{n} \cdot \frac{\partial P}{\partial \mathbf{n}}\right) \ .\end{aligned}$$

The Diffusion Matrix in Kirkwood Approximation

$D_{ij} = D_{||} n_i n_j + D_{\perp} (\delta_{ij} - n_i n_j)$ – diffusion matrix

$\mathbf{n} = (\cos(\phi), \sin(\phi))$- unit orientaional vector

$$D_{||} = k_B T \frac{\log(l/d)}{2\pi\eta_s l} - \text{parallel diffusion}$$

$$D_{\perp} = D_{||}/2 - \text{perpendicular diffusion}$$

$$D_r = k_B T \frac{12\log(l/d)}{\pi\eta_s l^3} - \text{rotational diffusion}$$

l – length of the rod, *d*- diameter, η_s – viscosity of solvent

Theoretical Model

- Microscopic interaction rules:

  -self-propulsion; inelastic collision

  -flow advection; direction realignment in shear flow

  -energy injection in the fluid due to swimming

$$\frac{\partial \rho}{\partial t} + \mathbf{v}\nabla\rho = D\nabla^2\rho - v_0\pi\nabla\boldsymbol{\tau}$$

$$\frac{\partial \boldsymbol{\tau}}{\partial t} + \mathbf{v}\nabla\boldsymbol{\tau} + \frac{1}{2}\Omega\times\boldsymbol{\tau} + \kappa u_{ij}\tau_j = (0.273\rho - 1)\boldsymbol{\tau} - 2.18|\boldsymbol{\tau}|^2\boldsymbol{\tau} - \frac{v_0}{4\pi}\nabla\rho + \frac{5\nabla^2\boldsymbol{\tau}}{192} + \frac{\nabla\nabla\cdot\boldsymbol{\tau}}{96}$$

$$\frac{\partial \mathbf{v}}{\partial t} + \mathbf{v}\nabla\mathbf{v} = \nu\nabla^2\mathbf{v} - \nabla p - \beta\mathbf{v} + \alpha\boldsymbol{\tau}, \nabla\mathbf{v} = 0, \Omega = \nabla\times\mathbf{v}$$

no-slip b.c. for the film

Ω- vorticity, p-pressure, ν-viscosity, v_0 -swimming speed

Results of Modeling

- *Instability of uniform flow*
- *Mechanism: coupling between self-propulsion and shear-induced alignment*

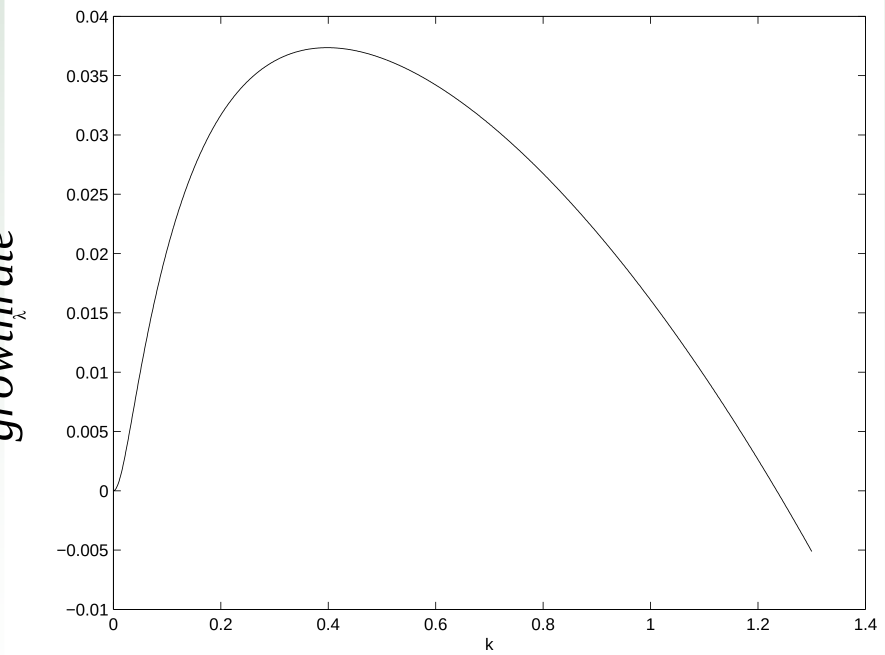

growthrate

wavenumber

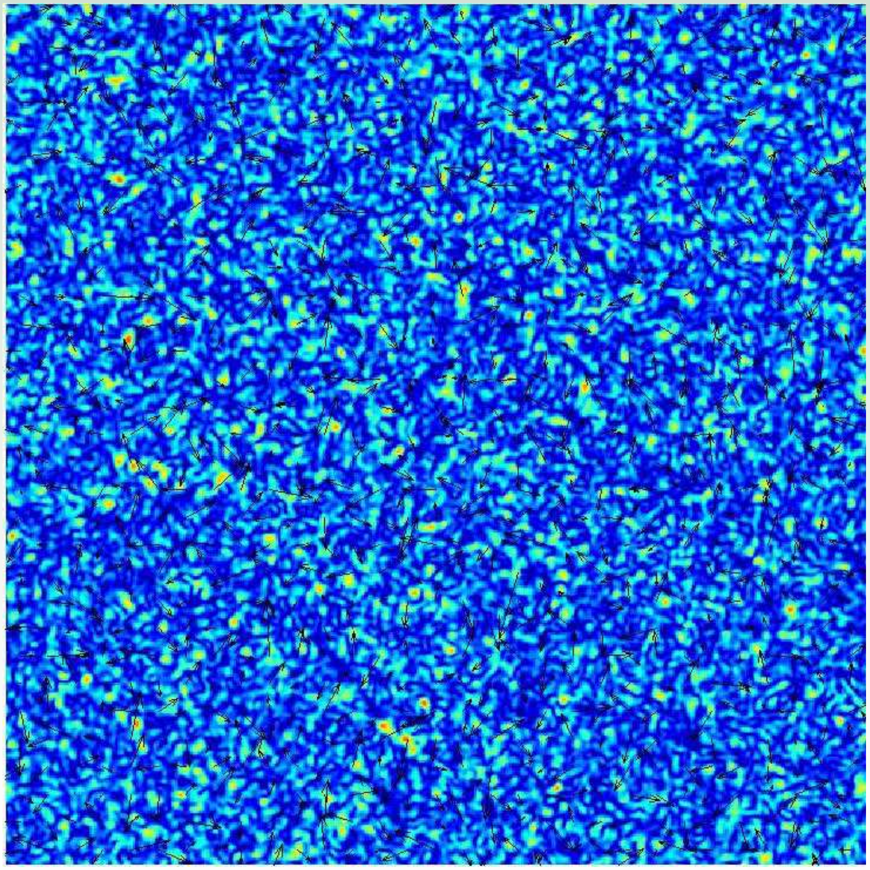

Experiment and Theory

Experiment

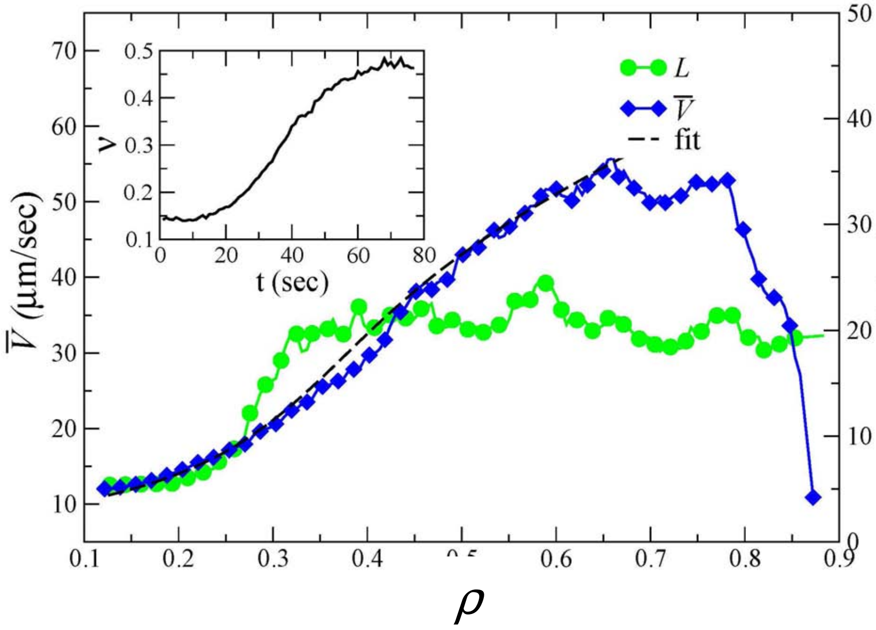

Theory

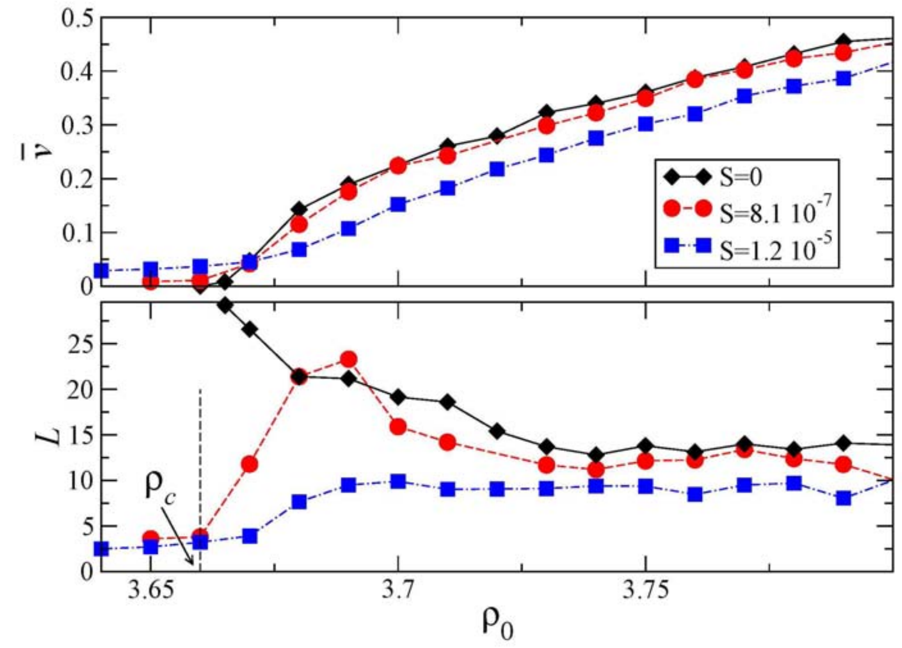

Swirling of apolar particles

- Vibrated monolayer of a elongated particles (rice, pins, cylinders)
- Vigorous high-frequency vibration (f ≈200 Hz, acceleration Γ~6 g)
- Flat tips: tetratic states
- Tapered tips: nematic, smectic order and dynamics states
- Swirling observed for rolling pins
- Mechanism? Boundary effects? Defects Motion?

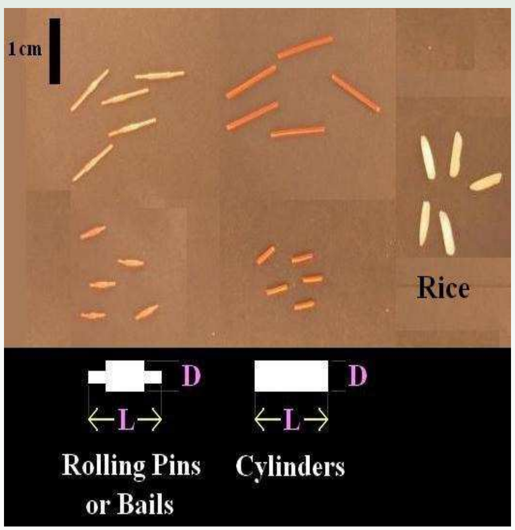

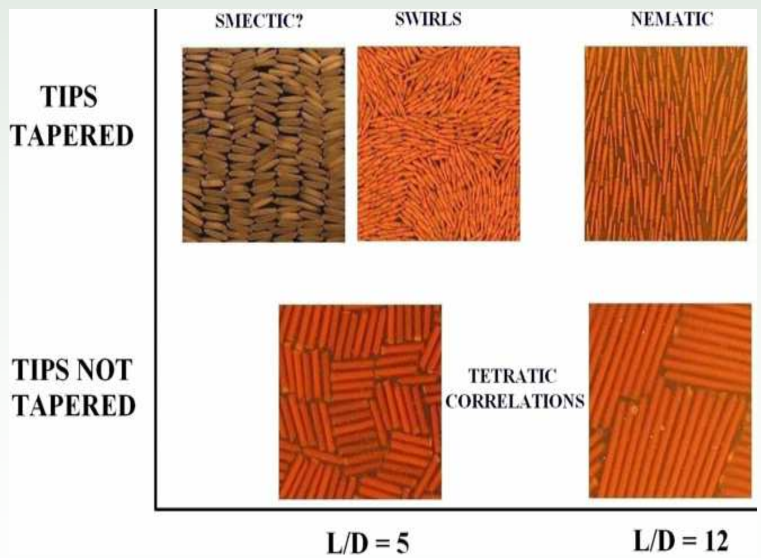

Narayan, Menon, Ramaswami, 2006

Swirling States: Apolar vs Self-Propelled Particles

Apolar bioparticles

Vibrated jasmine rice
freq f=129 Hz

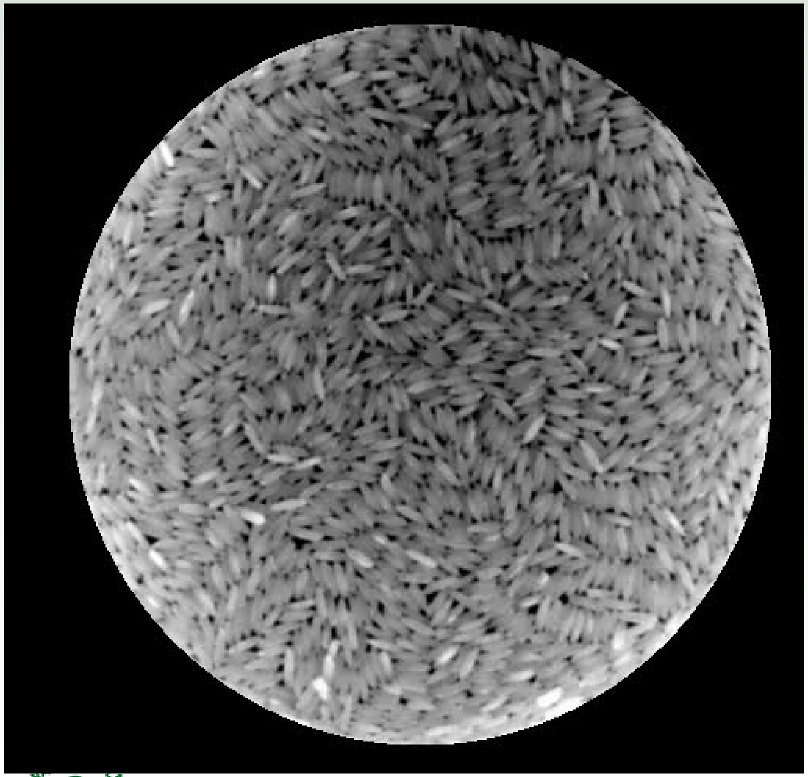

Active self-propelled particles

Swimming bacteria
Sokolov, Aranson, Goldstein, Kessler

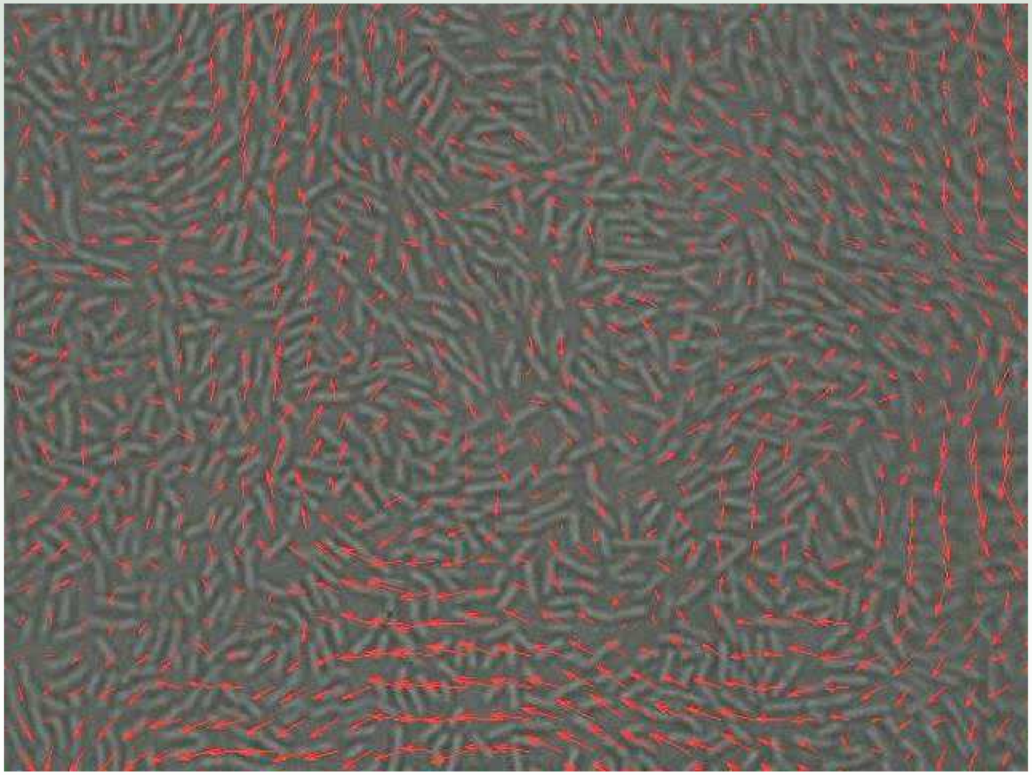

Schematics of experimental setup

- electromechanical shaker
- open air cell
- frequencies   f=100-200 Hz
- accelerations Γ=1.7-5 g

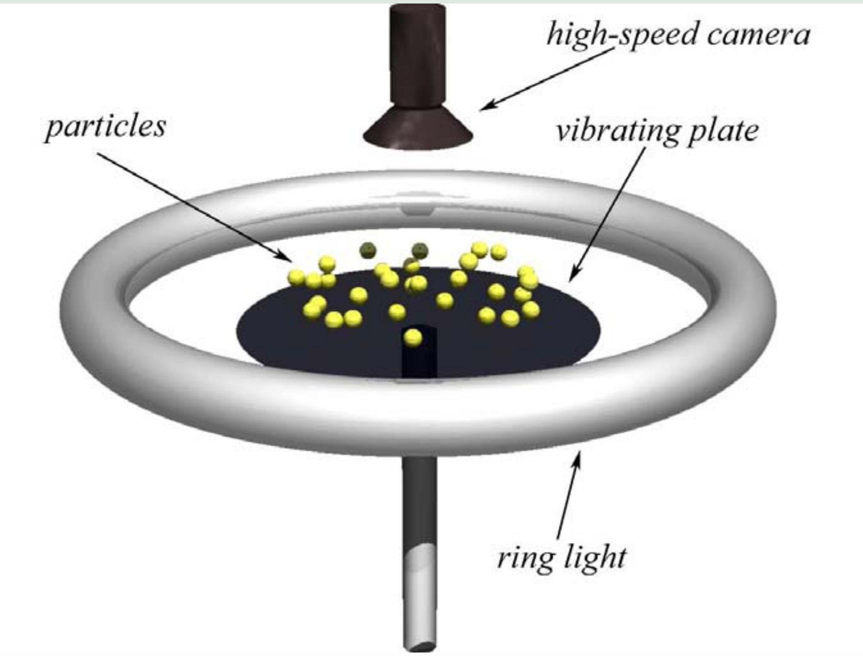

Particles

- sushi rice, aspect ratio L/d= 2
- jasmine rice, L/d = 3.5-4
- Basmati rice, L/d=6-8
- dowel pins, L/D=4
- mustard seeds, spherical

Techniques

- Particle tracking
- PIV
- 2 tri-axial accelerometers for all vibration components

Rigid-body rotation

- Fast-forward videos
- Resonance-like behavior at f=132 Hz
- Switching states
- Angular velocity increases with acceleration

Angular velocity ω vs f & Γ

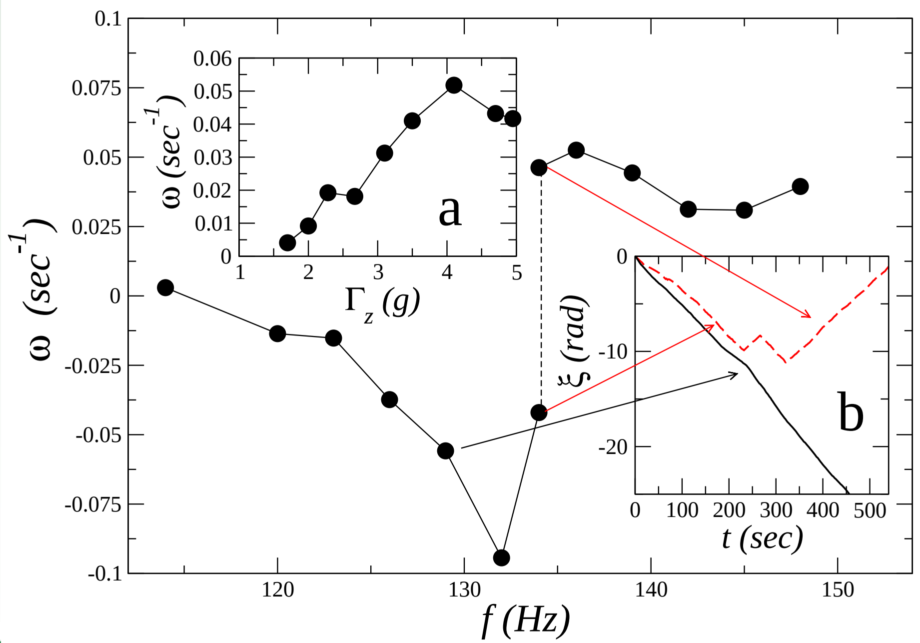

Swirling motion

- Rigid-body rotation superimposed with swirls
- Swirls become more pronounced with the decrease of rotation frequency

Jasmine rice, f=142 Hz, Γ=2 g, filling fraction about 80%

Raw PIV

Bulk rotation subtracted

Relative strength of swirls

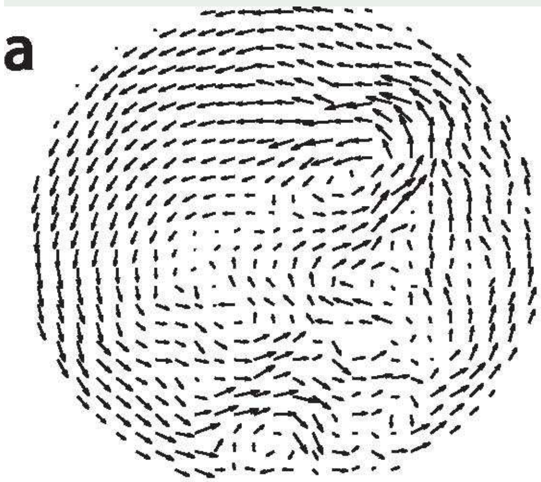

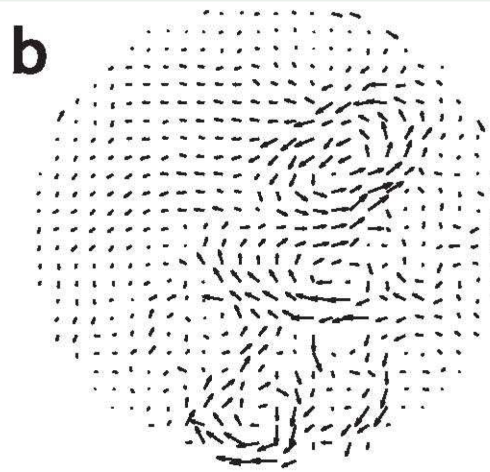

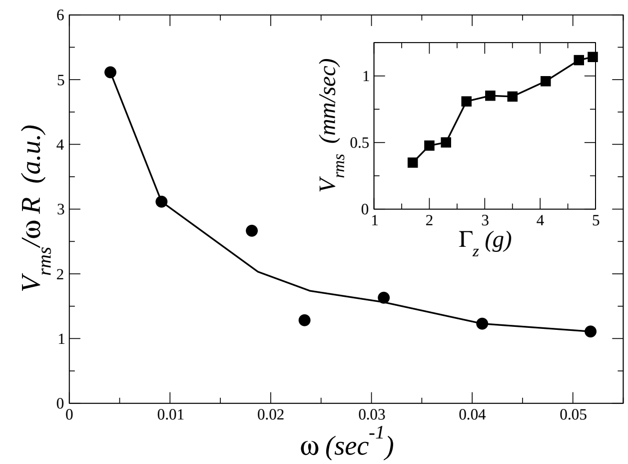

Horizontal acceleration – the main cause of the rotation

- Tangential Γ_t and normal Γ_n accelerations coincide in both locations
- Primary motion of plate: vertical vibration and twisting
- Resonance peak at f≈132 Hz (shaker specific)

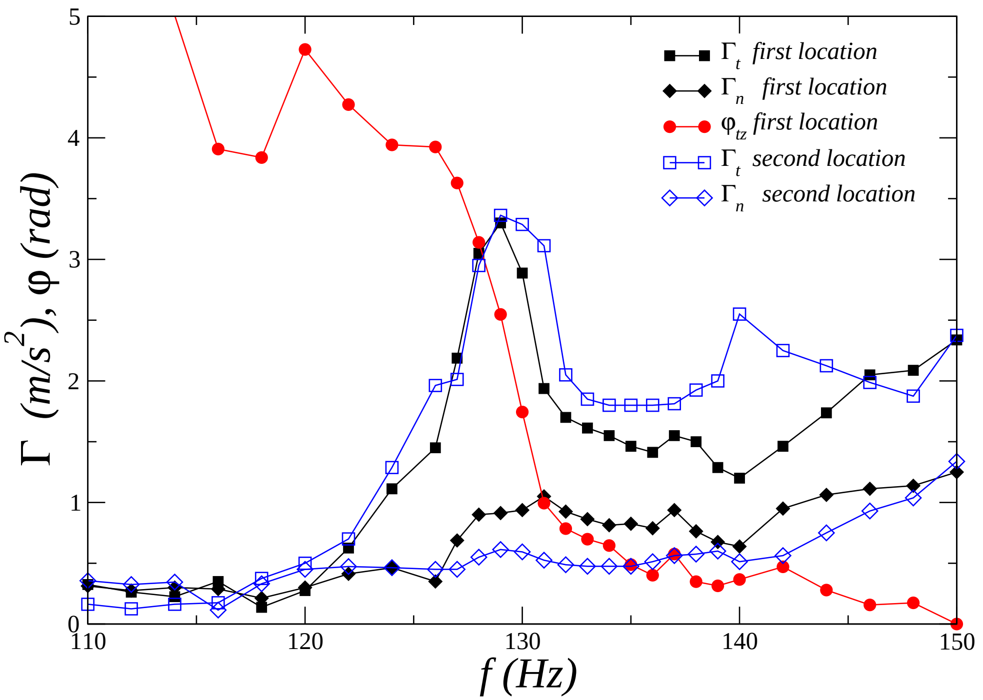

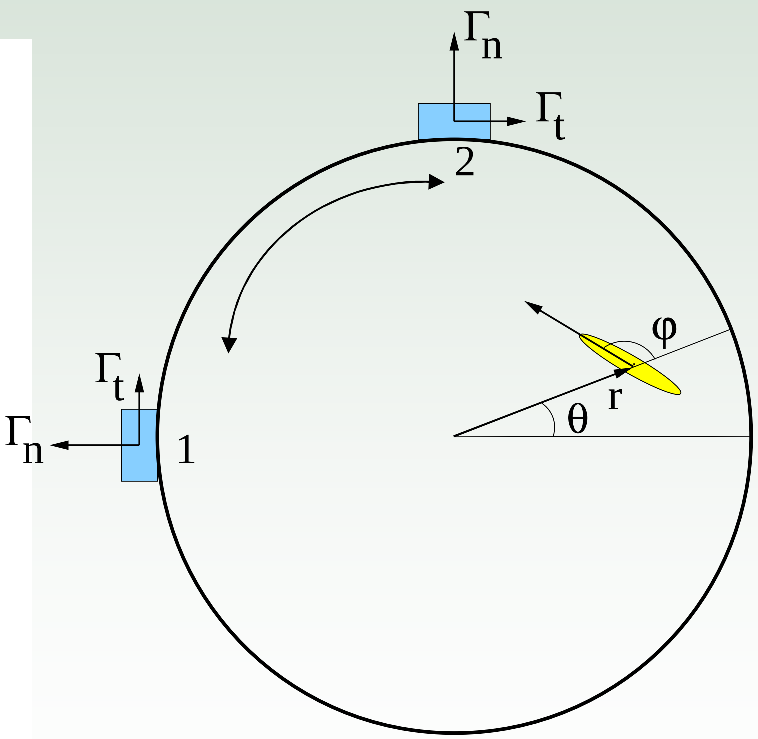

Properties of dilute gas of particles

- Experiments with a few grains only
- Extracted long trajectories
- Measured velocity vs angle φ
- Monomers and dimers (catamarans)
- Dynamics: diffusion and drift

$$\mathbf{B}\bullet\mathbf{V} = \mathbf{F}_0 + \xi(t) - \text{equation of motion}$$

$$\mathbf{B} = \beta_0 \mathbf{I} + \beta_1 \begin{pmatrix} \cos(2\varphi) & \sin(2\varphi) \\ \sin(2\varphi) & -\cos(2\varphi) \end{pmatrix}$$

$\xi(t)$ – white noise (from vibration)

B-anisotropic friction tensor

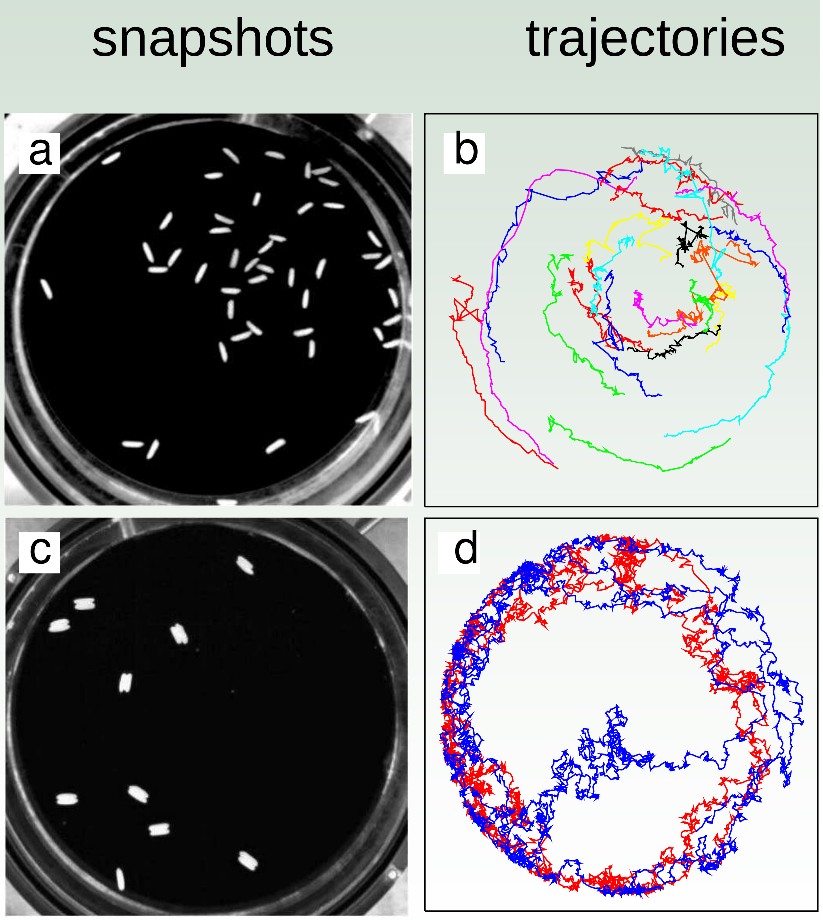

Anisotropic friction tensor

$$\langle V_\theta \rangle = \frac{F_0}{\beta_0}\left(1 - \frac{\beta_1}{\beta_0}\cos(2\varphi)\right) - \text{mean velocity vs angle}$$

$$\sigma_{V_\theta} = \sigma_0\left(1 - \frac{\beta_1}{\beta_0}\cos(2\varphi)\right); \sigma_{V_r} = \sigma_0\left(1 + \frac{\beta_1}{\beta_0}\cos(2\varphi)\right) - \text{dispersion } V_{r,\theta}$$

monomers

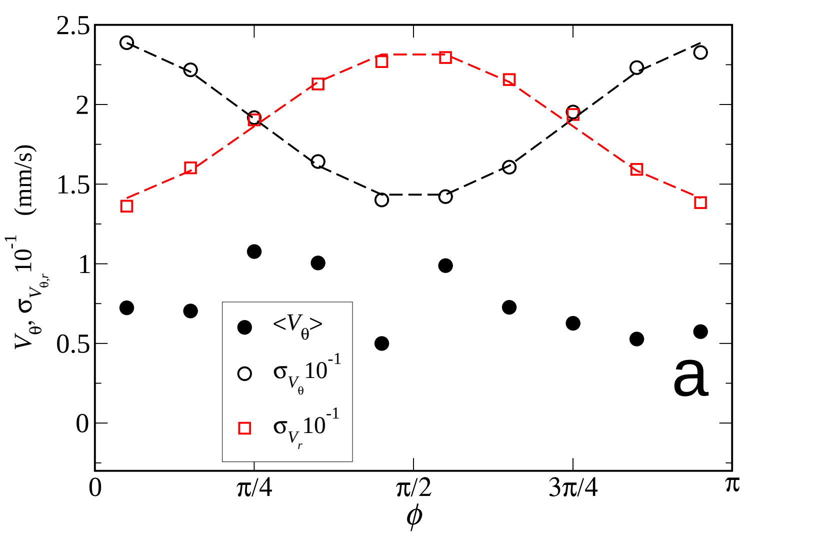

catamarans

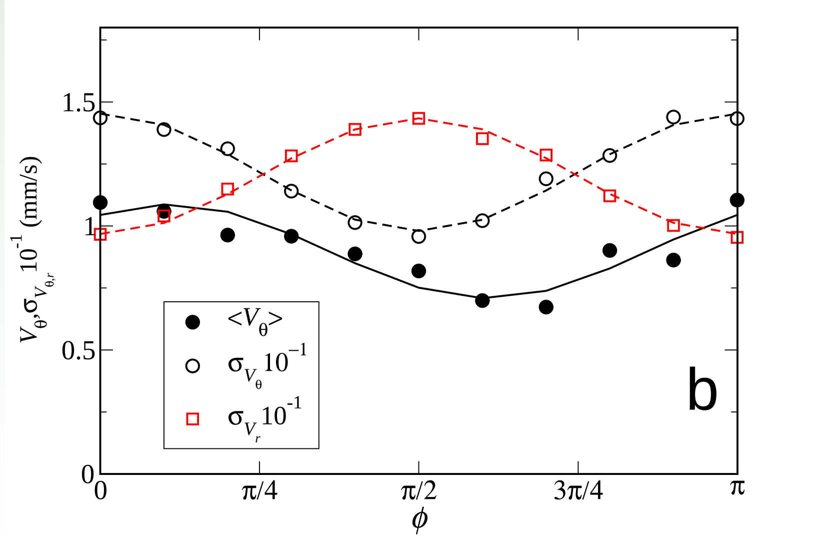

Theoretical Model

$$\mathbf{Q} = \frac{s}{2}\begin{pmatrix} \cos(2\varphi) & \sin(2\varphi) \\ \sin(2\varphi) & -\cos(2\varphi) \end{pmatrix} - \text{alignment tensor}, 0 < s < 1 \text{ - magnitude}$$

$\mathbf{v}$ – coarse-grained (hydrodynamic) velocity, $\mathbf{\Omega}$-vorticity tensor, p-pressure

$$\frac{\partial \mathbf{Q}}{\partial t} + (\nabla \mathbf{v})\mathbf{Q} = \varepsilon \mathbf{Q} - \frac{1}{2}\mathrm{Tr}(\mathbf{Q}\cdot\mathbf{Q})\mathbf{Q} + D_1 \nabla^2 \mathbf{Q} + D_2 \nabla\nabla\cdot\mathbf{Q} + \mathbf{\Omega Q} - \mathbf{Q\Omega}$$

$$\frac{\partial \mathbf{v}}{\partial t} + (\nabla \mathbf{v})\mathbf{v} = \eta \nabla^2 \mathbf{v} - \nabla p + \mathbf{F}(\mathbf{Q},\mathbf{v}), \nabla \mathbf{v} = 0$$

$$\mathbf{F}(\mathbf{Q},\mathbf{v}) = \mathbf{F}_0 - (\beta_0 - \beta_1 \mathbf{Q})\mathbf{v} - \text{anisotropic driving force}$$

Connection with the Ginzburg-Landau Model

Pseudo-orientation vector $\boldsymbol{\tau} = (\mathrm{Q}_{\mathrm{xx}}, Q_{xy}) = \frac{s}{2}\left(\cos(2\varphi), \sin(2\varphi)\right)$

Complex orientation $\psi = \tau_{\mathrm{x}} + i\tau_y = \frac{s}{2}\left(\cos(2\varphi) + i\sin(2\varphi)\right) = \frac{s}{2}e^{2i\varphi}$

$$\frac{\partial \boldsymbol{\tau}}{\partial t} + (\nabla \mathbf{v})\boldsymbol{\tau} = \varepsilon\boldsymbol{\tau} - |\,\boldsymbol{\tau}\,|^2\,\boldsymbol{\tau} + D_1\nabla^2\boldsymbol{\tau} + D_2\nabla\nabla\cdot\boldsymbol{\tau} + \boldsymbol{\Omega}\times\boldsymbol{\tau}$$

$$\frac{\partial \mathbf{v}}{\partial t} + (\nabla \mathbf{v})\mathbf{v} = \eta\nabla^2\mathbf{v} - \nabla p + \mathrm{F}_0\mathrm{x}_0 - \beta\mathbf{v} + \alpha\boldsymbol{\tau}, \nabla\mathbf{v} = 0$$

Relative strength of swirls exhibits similar behavior

Experiment

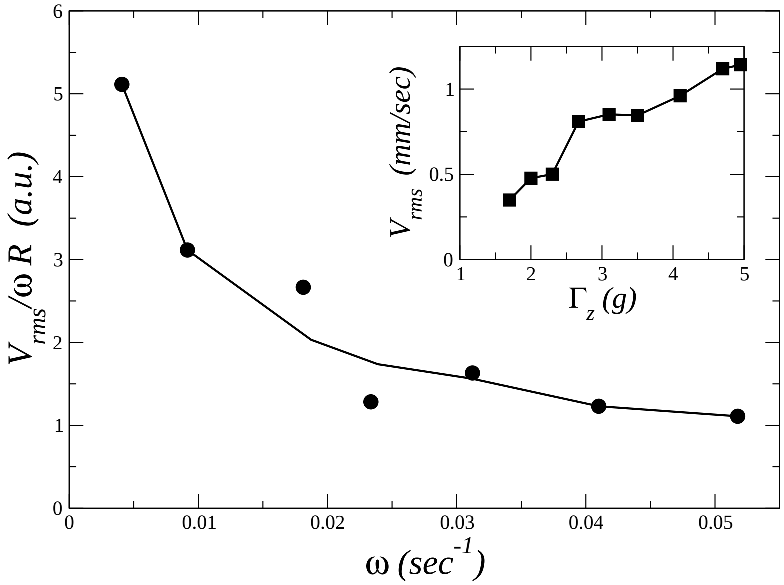

Theory

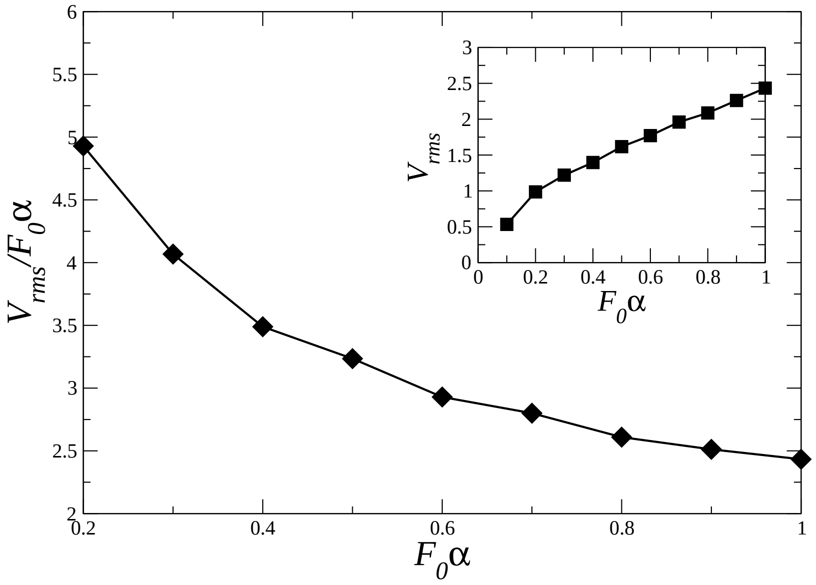

- ***Horizontal acceleration is cause of bulk rotation***
- ***Anisotropic friction is the cause of swirling motion***

Swirling motion: Theory

director field | velocity field

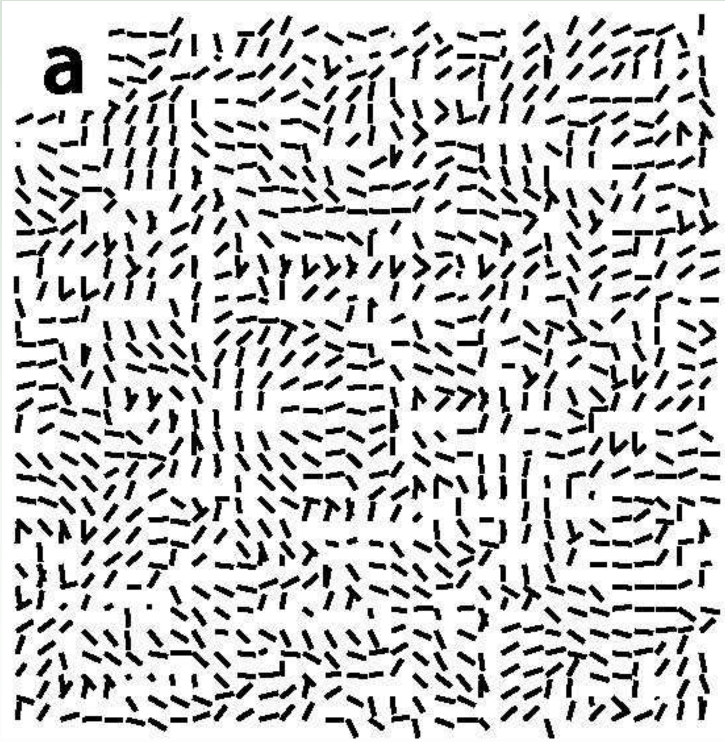

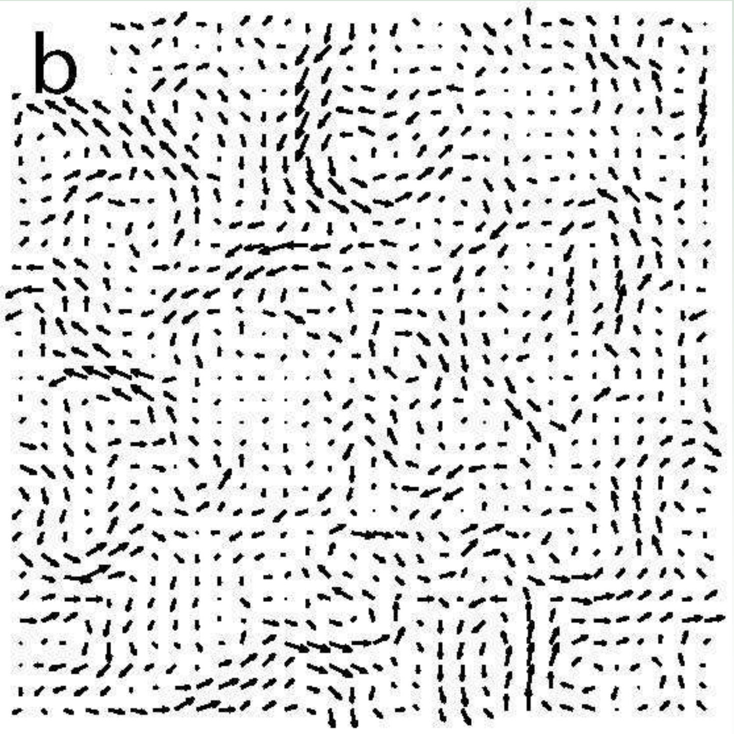

Conclusions

- Equations are derived from microscopic interaction rules
- Reasonable agreement with experiment
- Applications for biological and non-biological systems:

  -bacterial colonies

  -cytoskeleton dynamics

  -self-propelled particles (vibrated rods, etc)